Phil. Trans. R. Soc. Lond. A. **281**, 443–459 (1976) [443]
Printed in Great Britain

A.t.m. observations on the X u.v. emission from solar flares

By G. E. Brueckner
E. O. Hulburt Center for Space Research, Naval Research Laboratory, Washington, D.C. 20375, U.S.A.

[Plates 31–38]

Far ultraviolet spectroheliograms (190–465 Å) and ultraviolet spectra (900–1900 Å) of selected flares obtained on board Skylab by two instruments of the Naval Research Laboratory are presented. Time sequences of three events are discussed in detail; they are compared with simultaneous X-ray measurements from the N.R.L.'s Solrad 9 and from the OSO-7 X-ray spectrometer of the University of California, San Diego. In all events, where proper observational coverage was obtained, a small kernel seems to be the source of the prime energy release of a flare. The size of this kernel is determined by the spatial resolution of the spectroheliograph, which is approximately 2″. Densities in this kernel exceed 3×10^{12} cm^{-3}. Ion temperatures in a subflare kernel are determined to be larger than 20 MK. It is very likely, that these temperatures are much higher in the flare kernel of more energetic events. Hot clouds of coronal gas at 20 MK surround the kernel. These clouds are trapped below high magnetic structures, and subsequently seem to be the energy reservoir for heating the post flare loops. During the explosive phase, strong Doppler broadening can be seen, especially in transition zone lines of the brightened plages. These can be interpreted as impact of high energetic particles guided down to the solar surface along the loops. The observations suggest that high speed mass motions have their origin in the exploding flare kernel.

Introduction

It is the purpose of this paper, to summarize observations of selected solar flares obtained by the Naval Research Laboratory's two ultraviolet instruments on board Skylab. Three events will be discussed in detail: The 15 June 1973 flare, a small subflare of 9 August 1973, and the 21 January 1974 event. In addition, ultraviolet images of two other events will be shown to amplify findings in an attempt to sketch a general picture of a 'flare' as seen in the ultraviolet. The 15 June 1973 and the 9 August 1973 events have been selected because they would be the extremes as observed from Skylab with the N.R.L. instruments on a scale which would classify flares according to their explosive nature. The 15 June flare shows a strong explosive phase. Therefore, the secondary effects of a flare – heating of the corona, expulsion of material, formation of loops during the cooling phase – can be studied. But the explosive nature of the event obscures the primary energy source which is difficult to distinguish from the secondary effects. The 9 August subflare represents a class of events being confined to a small kernel, without explosions. This event is especially suited to study the primary energy producing process and the acceleration of particles. Because of its small size line profiles can be derived from slitless spectroheliograms which are not contaminated by spatial effects. There are indications that the same mechanism, responsible for the small event is also the prime energy source of the larger flare with the only difference, that in the latter case the catastrophic particle acceleration results in higher energies and a subsequent explosion. Particle energies are definitely higher in the 15 June event. Unfortunately the Skylab observations do not cover the 'flash' phase of both events. Therefore, a detailed discussion of the

21 January 1974 event has been included. Here, a series of spectroheliograms has been obtained by astronaut Dr E. Gibson, starting at the very beginning of the flare. The event can be called complex concerning all secondary effects of a flare, but it is the only one of all flares observed from Skylab, where the initial phase has been photographed by the N.R.L. spectroheliograph. Comparison will be made with Solrad 9 X-ray measurements and a hard X-ray burst in the 20–30 keV range measured by the X-ray detector on board OSO-7 of the University of California, San Diego. It will be finally tried to give a common description of different flares as seen in the ultraviolet.

The instrument

Slitless spectroheliograms are used, obtained by the N.R.L. spectroheliograph on board Skylab. The spatial resolution of the instrument in the wavelength regions, used for this analysis, can be estimated to be approximately 2–3″. With a linear dispersion of 1.35 Å mm^{-1} this results in a spectral resolution of 0.026 Å (30 km s^{-1}) for a point source.

The spectra in the wavelength region 1000–1950 Å simultaneously photographed by the N.R.L. Skylab spectrograph have a spatial resolution of 2″ × 60″ (slit-width × slit-length) (Bartoe, Brueckner, Purcell & Tousey 1974). Despite the fact that the spectrograph does not offer stigmatic imaging along the slit, structures perpendicular to the dispersion can be seen in these flare spectra, indicating the point source nature of most flare features. This will become especially clear, when spectra are compared with simultaneously photographed spectroheliograms. A spectral resolution of 0.07 Å full width at half maximum (corresponding to 14 km s^{-1} at 1500 Å) could be achieved, including the instrumental, film and microdensitometer effects.

Emission lines used for this analysis

In table 1 those emission lines are listed, which seem to have a more or less certain identification and hence will be used in the following dicussion of the ultraviolet appearance of solar flares. The selection of the lines was made in order to cover a wide range of ionization temperatures. An effort has been made, to discuss only flare images of different lines located close to the normal of the Wadsworth spectroheliograph to compare only images having approximately the same spatial resolution. However, a brief discussion of the identifications listed in table 1 seems appropriate, because some identifications must be called preliminary.

Fe XXIV ($2sg\,^2S–2p^2P^0$) at 192.0 Å (1/2–3/2) and at 255.07 Å (1/2–1/2) has been first identified by Neupert (1971 *a*) and later confirmed by Purcell & Widing (1972). The accurate wavelength of these two lines can be derived only in a statistical way, because the Fe XXIV emitting plasma often varies in its spatial location from the plasma emitting at the lower ionization stages, of which lines must be used as comparison standards and laboratory measurements of the Fe XXIV transitions do not exist. Six different flares have been investigated. The above values are the mean wavelength of 6 disk flares. Two limb flares have been excluded because the large shifts of the Fe XXIV lines relative to lower stages of ionization lines indicate, that the Fe XXIV in these limb events originates 17 000 km (the 2 December 1973 flare) and 34 000 km (the 16 December 1973 flare) above the limb. (In the case of the disk flares 15 June and 9 August, it is difficult to use the deviation from the main wavelength as a heights measure. It is impossible to distinguish horizontal from vertical displacements.)

Fe XXIII ($2s^2g\,^1S–2s^22p^3P^0_1$) at 263.81 Å has been predicted by Kononov, Koshelev & Podobedova (1974) and identified by Widing (1975) and Sandlin *et al.* (1975) in the N.R.L. Spectroheliograms of flares. The Fe XXIII emission originates from the same regions where Fe XXIV can be seen. A

strong support of the identification can be derived from the facts that the line does exist only in flares, its intensity follows generally that of the Fe XXIV emission, its spatial distribution is similar to the Fe XXIV emission, its apparent wavelength shifts follow those of the Fe XXIV emission in all events and its line profiles show a similar half-width. (The above given wavelength has been derived also as a mean of 6 cases, as outlined earlier for the Fe XXIV lines.) Fe XXI at 1354.1 Å ($2s^22p^2(^3P_1–^3P_2)$) has been identified by Doschek *et al.* (1975). It is another example of a line emitted by a highly ionized ion, which originates only in flares. (For a detailed discussion of this line see Brueckner (1974).) The same is true for lines of Fe XIX at 1118.4 Å ($2s^22p^4(^3P_2–^3P_1)$) and Fe XVIII at 974 Å ($2s^22p^5(^2P_{\frac{3}{2}}–^2P_{\frac{1}{2}})$), identified in the N.R.L. Skylab flare spectra (Doschek *et al.* 1975).

TABLE 1

λ Sun obs. Å	λ lab. Å	ion	transition	J–J	remarks	lg T_e
192.00	?	Fe XXIV	$2sg^2S–2p^2P^0$	1/2–3/2	—	7.25
192.82†	192.819	Fe XI	$3p^4g^3P–3p^3(^2D^0)3d\ ^3P^0$	1–2	—	—
192.82	—	Ca XVII	$2s^2g^1P–2s2p^1P^0$	0–1	—	—
237.39†	237.39	He II	—	—	—	—
240.78	240.713	Fe XIII	$3s^23p^2g^3P–3s3p^3\ ^3S^0$	0–1	—	6.2
241.88	241.739	Fe IX (?)	$^1S_0–^3P_2$	—	—	5.85
242.28	—	Ar XIII	$2s^22p^2g\ ^3P–2s\ 2p^3\ ^3D^0$	1–2	—	—
243.03†	243.03	He II	—	—	—	—
243.86	243.783	Fe XV	$3p^2\ ^3P–3p3d\ ^3D^0$	2–3	—	6.3
244.90	244.912	Fe IX	$^1S_0–^3P_1$	—	—	5.85
246.21	246.210	Fe XIII	$3s^23p^2g^3P–3s3p^3\ ^3S^0$	1–1	—	6.2
248.50	—	Ov	$2s2p^1P^0–2s3s^1S$	1–0	—	5.3
248.71	248.68	Ar XIII	$2s2p^2g^3P–2s2p^3\ ^3D$	2–3	—	—
249.20	249.18	Ni XVII	$3s^2g^1S–3s3p^1P^0$	0–1	—	6.4
249.42	249.46	Ar XIII	$2s2p^2g^3P–2s2p^3\ ^3D^0$	2–2	—	—
251.09	—	Fe XVI	$3p^2P^0–3d^2D$	1/2–3/2	—	6.4
251.95	251.949	Fe XIII	$3s^23p^2g^3P–3s3p^3\ ^3S^0$	2–1	—	6.2
252.25	252.19	Fe XIV	$3s^23pg^2P–3s3p^2\ ^2P$	1/2–3/2	—	6.3
255.07	?	Fe XXIV	$2sg^2S–2p^2P^0$	1/2–1/2	—	7.25
256.32†	256.32	He II	—	—	—	—
256.63	256.569	Si X	$2s^22pg^2P^0–2s2p^2\ ^2P$	1/2–1/2	blend	6.1
257.30	257.37	Ar XIV	$2s^22pg^2P^0–2s2p^2\ ^2D$	3/2–5/2	blend Fe XIV	—
258.29	258.347	Si X	$2s^22pg^2P^0–2s2p^2\ ^2P$	3/2–3/2	—	6.1
261.01	261.045	Si X	$2s^22pg^2P^0–2s2p^2\ ^2P$	3/2–1/2	—	6.1
262.98†	262.98	Fe XVI	$3p^2P^0–3d^2D$	3/2–5/2	—	6.4
263.81	?	Fe XXIII	$2s^2g^1S–2s2p^3P_1{}^0$	0–1	—	7.2
264.799†	264.799	Fe XIV	$3s^23pg^2P–3s3p^2\ ^2P$	3/2–3/2	—	6.3
284.15†	284.15	Fe XV	$3s^2g^1S–3s3p^1P^0$	0–1	—	6.3
335.407†	335.407	Fe XVI	$3sg^2S–3p^2P^0$	1/2–3/2	—	6.4
368.071†	368.071	Mg IX	$2s^2g^1S–2s2p^1P^0$	0–1	—	6.0
465.221†	465.221	Ne VII	$2s^2g^1S–2s2p^1P^0$	0–1	—	5.7‡

† Used as wavelength standards.
‡ The electron temperatures in table 1 have been taken from Jordan (1969, 1970).

Ni XVII ($3s^2g^1S–3s3p^1P^0$) at 249.20 Å has been identified by Widing, Sandlin & Cowan (1971) in the first N.R.L. slitless flare spectroheliogram (Tousey 1971). Its strong appearance in all flare kernels discussed in this paper matches very well the behaviour of the nearby Fe XVI line at 251.09 Å ($3p^2P^0–3dD$) as well as the Fe XVI line at 262.98 Å ($3p^2P^0–3d^2D$). Both ions have a maximum abundance at approximately 3×10^6 K.

Ca XVII ($2s^2g^1P–2s2p^1P^0$) at 192.82 Å was identified by Purcell & Widing (1972) in the same N.R.L. slitless flare spectroheliogram mentioned above. This line may be blended in the corona with Fe XI line at 192.84 Å ($3p^4g^3P–3p^3(^2D^0)3d^3P^0$) identified in the quiet Sun by Firth *et al.* 1974.

But from time sequences of flare spectroheliograms discussed later one can conclude that the majority of the emission in the hot flare kernels is caused by the Ca XVII line.

As will be noted later, there is a distinct difference in the time behaviour of Fe XIII and Fe XIV compared with Fe XVI in a flare kernel. Also all loops, seen at the limb, are sharper in Fe XIII and Fe XIV when compared with Fe XVI (see figure 21). This makes the identification of Fe XIV at 252.25 Å ($3s^2 3pg\,^2P–3s3p^2\,^2P$) (1/2–3/2) and Fe XIV at 264.799 Å (same transition) (3/2–3/2) as well as that of the Fe XIII lines at 240.78, 246.21, 251.95 (transitions see table 1) certain (Widing *et al.* (1971)).

The Ar XIII lines ($2s2p^2g\,^3P–2s2p^3\,^3D^0$) at 242.28 Å, 248.68 Å and 249.46 Å behave like cooler ions of Fe XIII and Fe XIV. Identification of the 242.28 Å and 248.68 Å lines has been made by Purcell & Widing (1972).

Three lines of Si X at 256.63 Å, 258.29 Å, and 261.01 Å are present in the flare kernels, becoming strong during the cooling phase. They have been identified in the quiet Sun by Firth *et al.* (1974).

In the quiet Sun, the intercombination lines of Fe IX at 241.74 Å ($^1S_0–^3P_2$) and at 244.91 Å ($^1S_0–^3P_1$) have been identified by Firth *et al.* (1974). It remains very questionable whether these identifications can be applied to flares. A strong feature exists in flare kernels and in post-flare loops at 244.86 Å, but nothing at 241.74 Å in kernels, yet the 241.74 Å transition should be twice as strong as the 244.91 Å transition. A weak feature at 241.74 Å can be seen only in post-flare loops, but they are definitely much weaker in the short wavelength transition ($^1S_0–^3P_2$) than in the long wavelength transition ($^1S_0–^3P_1$), contrary to the predicted intensity ratio.

All other lines discussed in this paper have long established identifications which do not need any further discussion.

The 2-B flare of 15 June 1973

This flare was the largest flare, covered by the N.R.L. Skylab instruments. One can categorize the observations into 4 phases: The preflare phase, the flash phase, the explosive phase and the cooling phase.

Several spectroheliograms, taken before the flare onset at 5h08, 12h18 and 13h52 are available. Figure 1, plate 31, shows the appearance of the corona in Fe XV and Fe XVI above the whole active region with emphasis of the outer pherephiral areas, while the core of the active region is overexposed. One notes a change between 5h08 and 14h11 in the lower SE area, relocations of loops can be clearly seen. Also a depletion of the strong loop system extending toward the north (top) takes place. The latter effect can be seen more clearly in figure 2, plate 31 which shows coronal images of the central loop and plage system in Fe XV and Fe XVI. These effects may have nothing to do with the flare, relocations of loops on a time scale of hours are common features in active regions as shown recently by Sheeley *et al.* (1975). Figure 3, plate 32, shows the central core of the active region in Fe XV and Fe XVI where the flare occurred. Thirteen minutes before flare onset which is defined at 14h5 min by the first type III burst an inconspicuous plage area seems to be equally bright in Fe XV and in Fe XVI, while shortly after the flare onset Fe XVI is much more intense than Fe XV, which indicates a sudden heating of the central plage area and the adjacent loops toward the southwest. Before the flare a growing absorption feature in Ne VII and Mg IX (figure 4, plate 32) as well as in Fe XV and Fe XVI can be seen, located at the centre of the active region. U.v. absorption is typical of all filaments, caused either by the absorption in continua or by the absence of hot emission in the transition zone and coronal lines.

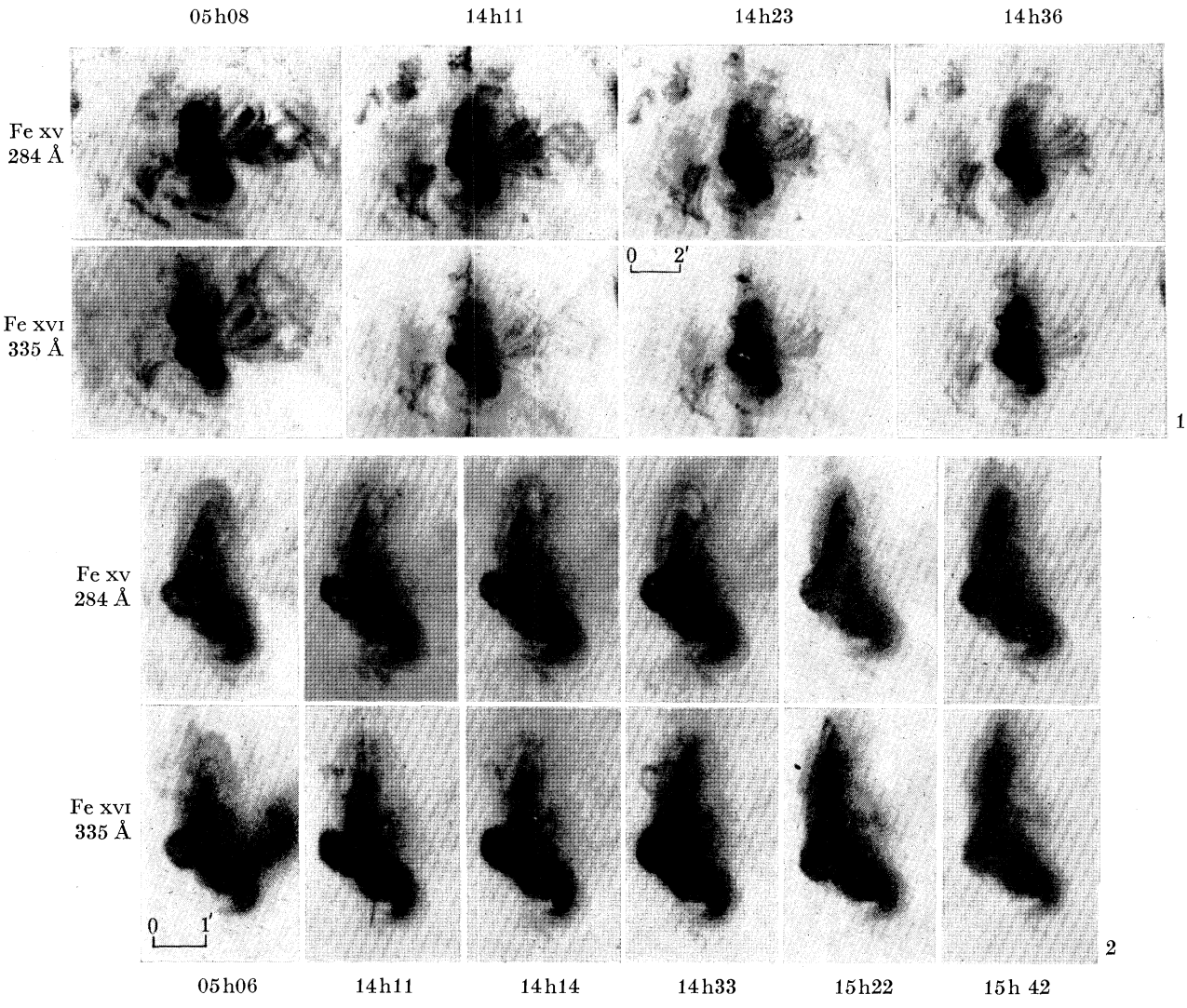

FIGURE 1. Development of the active region, in which the 15 June 1973 flare occurred as seen in Fe xv 284 Å and Fe xvi 335 Å.

FIGURE 2. The central plage and loop system before, during and after the 15 June 1973 flare; Fe xv 284 Å and Fe xvi 335 Å.

(*Facing p.* 446)

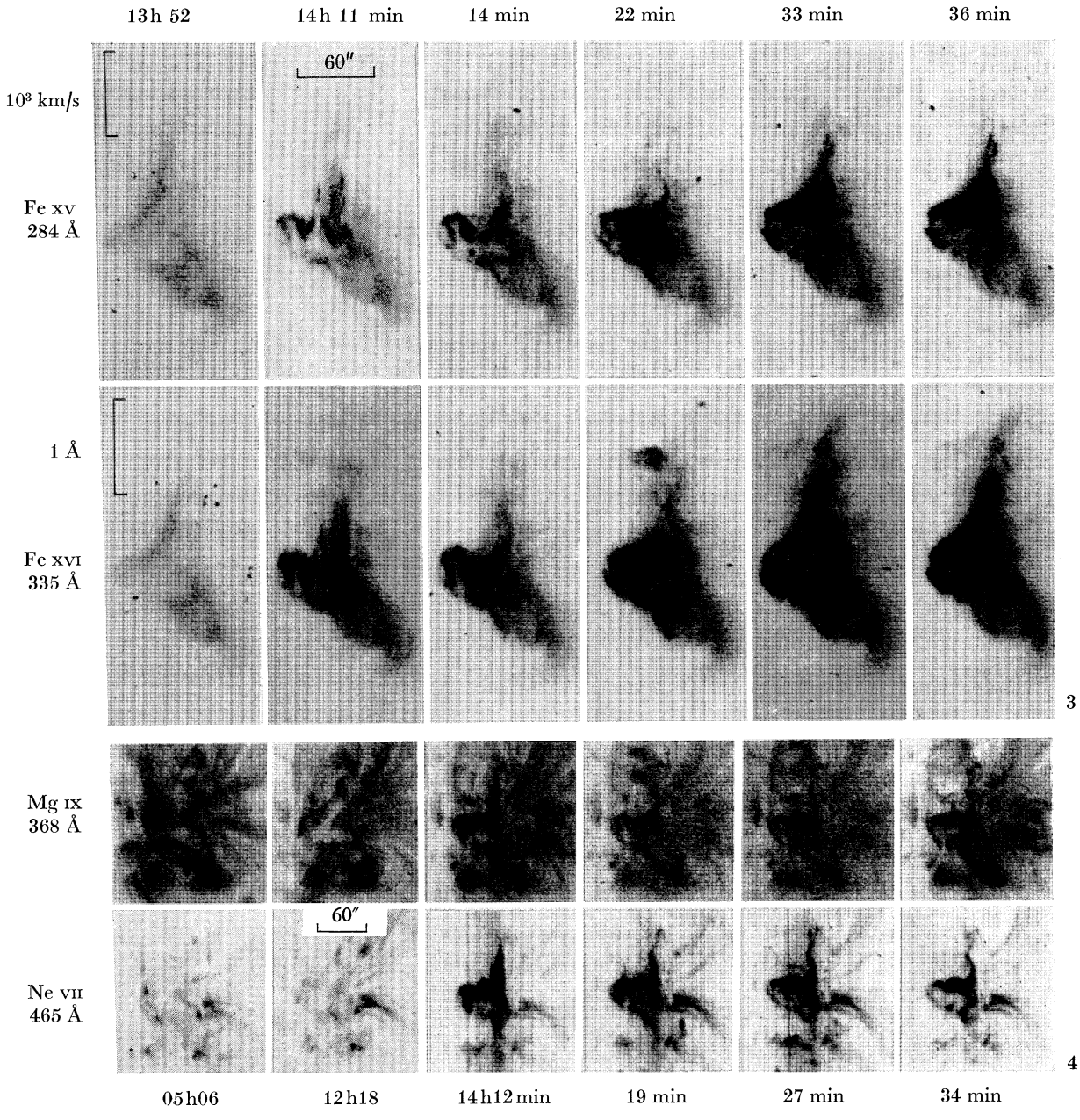

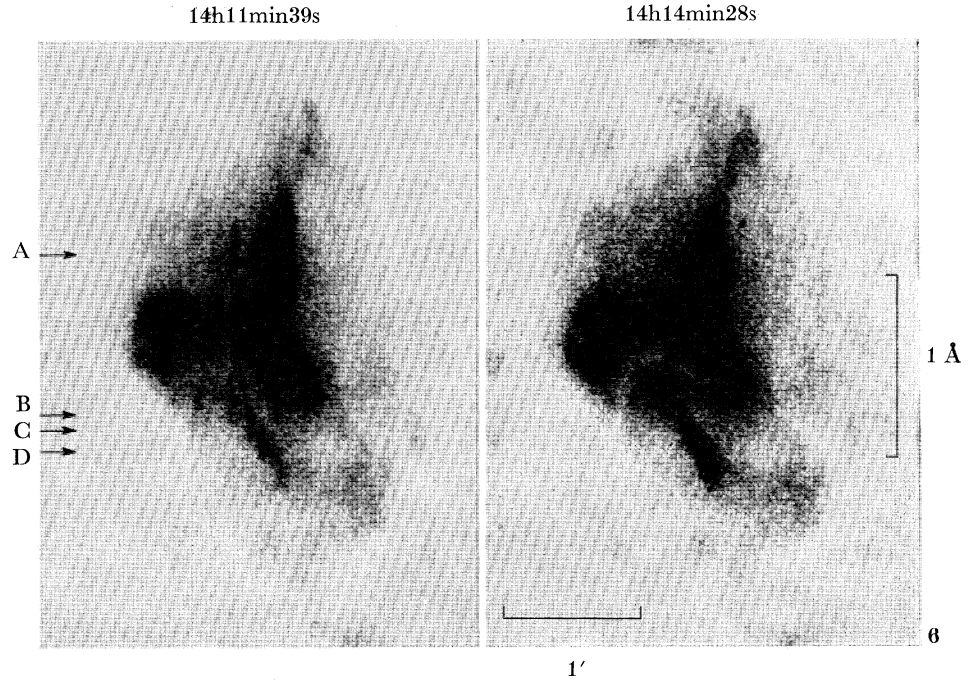

FIGURES 3, 4 AND 6. For description see opposite

Ne VII usually identifies the footprints of the loops and their lower, cooler and denser part. One notes distinguished changes between 5h08 U.T. and 12h18 U.T. (figure 4); whether they are typical of any preflare development cannot be proven.

The first series of flare spectroheliograms were obtained at 14h11 U.T., approximately 6 min after flare onset. They do not cover the flash phase and are only representative of the latter part of the explosive phase. As pointed out before the entire plage and some loop systems are heated at this moment. (Figure 3, Fe XV and Fe XVI for comparison at 14h11.) Fe XV, Fe XVI, Fe XXIV and He II images of the explosive phase of the flare are shown in figure 5, plate 33, at two different times (0 and 8.25 s). Another set of images taken 160 s later when the explosive phase has ceased has been added for comparison. Unfortunately, the images at 0 and 8.25 s have been taken with different exposure times (2.5 and 10 s respectively). It is clear that the narrow features, indicated by an arrow at *A* is moving, as seen from its Doppler shift Δl. The projected velocity can be measured to be 1100 km s^{-1}. It is conspicuous, that this feature is lined up along the direction of dispersion with a gap in the very intense bridge, which may indicate its origin. But it should be pointed out, that the size of this very fast moving feature is given by the resolution of the instrument. Its elongation along the direction of dispersion must be caused by Doppler shifts and dislocation during the duration of the exposure.

Other small discrete broadened emission features are indicated by an arrow at *C*. Here we do not see dislocations within the 8.25 s between exposures 1 and 2. But it is conspicuous, that nothing very bright is left at their location on exposure 3, 160 s later. They may be therefore interpreted as clouds, moving along or close to the direction of sight with high velocities and therefore Doppler shifted. A very bright streak, indicated by an arrow at *B* seems to be a feature elongated along the direction of dispersion, originating also at the very turbulent bridge. It is conceivable, that this streak is the picture of a blast wave of material moving out with a wide range of velocities up to 500 km s^{-1}, indicated by its Doppler shift. It has disappeared on the exposure taken 160 s later. It is conspicuous, that all these features seem to originate from a single small point at the centre of the active region, above which the hot Fe XXIV cloud is located.

If one wants to determine the exact location of this cloud, relative to the other images, one must take into account the wavelength difference, Doppler effects and spatial dislocation. From the 3 images in figure 5 it is obvious that the cloud is moving, therefore its location relative to the other images can only be estimated. But there seem to be no lateral movements relative to the direction of dispersion, which indicates that the cloud's dislocation along the direction of dispersion is caused by Doppler shifts. Laterally the Fe XXIV cloud seems to be located exactly above the area in the Fe XV, Fe XVI and He II images, where the most violent Doppler-motions can be seen.

Figure 6, plate 32, shows the He II 304 Å plage during and after the explosive phase of the flare. The arrows at *B*, *C*, and *D* point to small, Doppler broadened features along a narrow ribbon of

---

Description of plate 32

Figure 3. Development of the 15 June 1973 flare, exposed for the brightest portions of the plages and loops; Fe XV 284 Å and Fe XVI 335 Å.

Figure 4. Development of the active region, in which the 15 June 1973 flare occurred as seen in Mg IX 368 Å and Ne VII 465 Å

Figure 6. He II 304 Å images of the plage during and after the explosive phase of the 15 June 1973 flare.

the plage. During the explosive phase, the entire ribbon seems to consist of discrete, Doppler broadened emission points, while afterward a strong but blurred emission prevails. The Doppler broadened small points can be seen best along the ribbon, but from the overall appearance of the plage during and after the explosive phase one has the impression, that the whole plage is Doppler broadened during the explosive phase because it seems to be elongated along the direction of dispersion. One may speculate that the whole plage consists of very small, bright, Doppler broadened points which are not resolved in most of the plage areas. Slit spectra of the active region taken simultaneously with the spectroheliograms will give further evidence that the plage area consists of small, Doppler broadened emission points.

Images of the inner flare region in many emission lines are shown in figure 7, plate 34. While most of the coronal lines seem to outline the plage and the loop structure above it, the very hot emission from Fe XXIV and Fe XXIII is distinctly different. The formation of postflare loops seems to start when the hot Fe XXIV cloud is disappearing.

During the subsequent cooling phase,† apparently new loops are forming, as can be seen in figure 7, emitting first in hotter ions, like Fe XVI and later in cooler ions like Fe XIV. It could be speculated, that the very hot Fe XXIV emitting plasma serves as a reservoir for the energy needed to heat these loops. It should be emphasized that we may not see the formation of new loops, rather the heating and subsequent cooling of already existing loop formation which are not dense enough prior to the injection of flare energy to be seen. These post-flare loops have been detected by Bruzek (1962) emitting in forbidden lines of highly ionized atoms in the visible spectrum and sometimes in Hα.

The Fe IX images (figure 7) are different from all other coronal pictures. Here the contrast between the very small Doppler broadened kernels and the surrounding area seems to be more pronounced. It may be, that this effect is true for all cooler lines, emitted at temperatures between 10^5 and 10^6 K but cannot be seen clearly in the Ne VII and Mg IX images because they are over-exposed (see figure 4). (The identification problem of Fe IX as mentioned in an earlier section remains unanswered. It should be pointed out, that the other Fe IX line at 241.74 Å, which should be twice as strong, does not exist in the dense, Doppler-broadened portions of the plage.)

Slit spectra of the 15 *June flare*

The spectra obtained by the Naval Research Laboratory's spectrograph simultaneously with the spectroheliograms, have been discussed in detail elsewhere (Brueckner 1974). Therefore, only a summary is given here.

Figure 8, plate 33, shows the position of the spectrograph slit across the Hα flare as seen in the on board Hα display. The spectrograph is not stigmatic along the slit, the spectra therefore are averaged over all profiles of discrete features which are covered by the slit.

A time sequence of the 15 June flare spectra is shown in figure 9, plate 35. These spectra are characterized by the general enhancement of all neutral chromospheric emission lines without distinguishable profile changes, only saturation effects change the profiles slightly. Examples being Ly-α and the O I resonance triplet at 1300 Å. All ionized lines like Si III at 1206 Å and N V at 1238 and 1242 Å show strong broadening and large shifts of the line profiles. These broadenings and shifts last throughout the explosive phase of the flare until 14h18, at which time they suddenly disappear. Most influenced by line broadening and shifts are the medium ionized lines,

† The term cooling is used here only for the originally very hot trapped coronal gas as outlined by the Fe XXIV cloud.

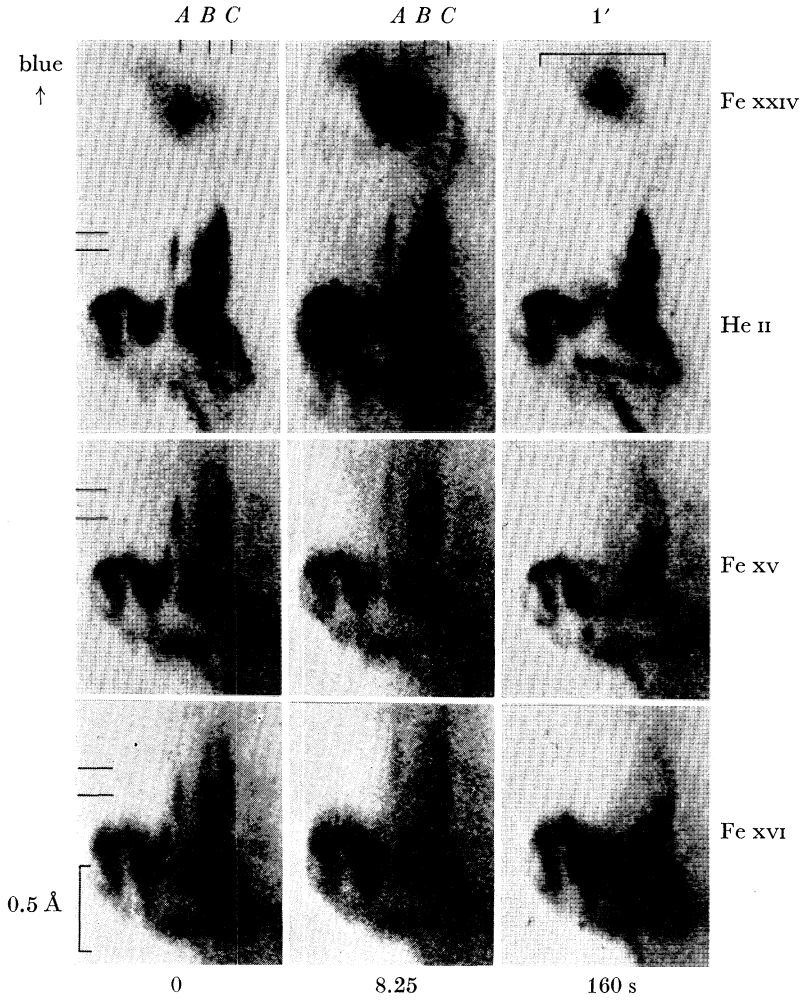

FIGURE 5. Rapid changes of 15 June 1973 flare images in Fe xv 284 Å, Fe xvi 335 Å, He ii 256 Å and Fe xxiv 255 Å. Zero seconds corresponds to the time, when the first flare spectroheliogram was taken. At 160 s the explosive phase of the flare has ceased. (The images at 0 s and 160 s are 2.5 s exposure, the images at 8.25 s 10 s exposures.) The parallel lines on the left hand photos indicate Δl.

FIGURE 8. Position of the spectrograph slit on the 15 June 1973 flare Hα image. The slit was located along the vertical cross-hair.

(*Facing p.* 448)

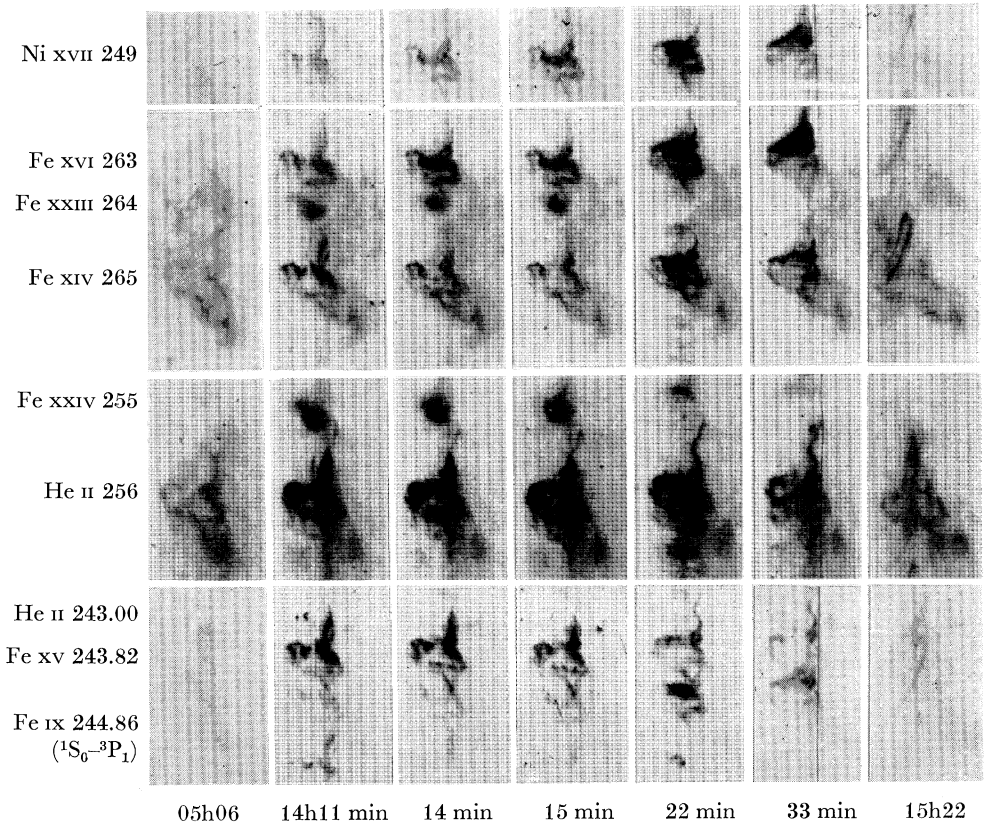

FIGURE 7. Time sequences of 15 June 1973 flare images in Ni XVII 249 Å, Fe XVI 263 Å, Fe XXIII 264 Å, Fe XIV 265 Å, Fe XXIV 255 Å, He II 256 Å, He II 243 Å, Fe XV 243.82 Å and Fe IX (?) 244.86 Å.

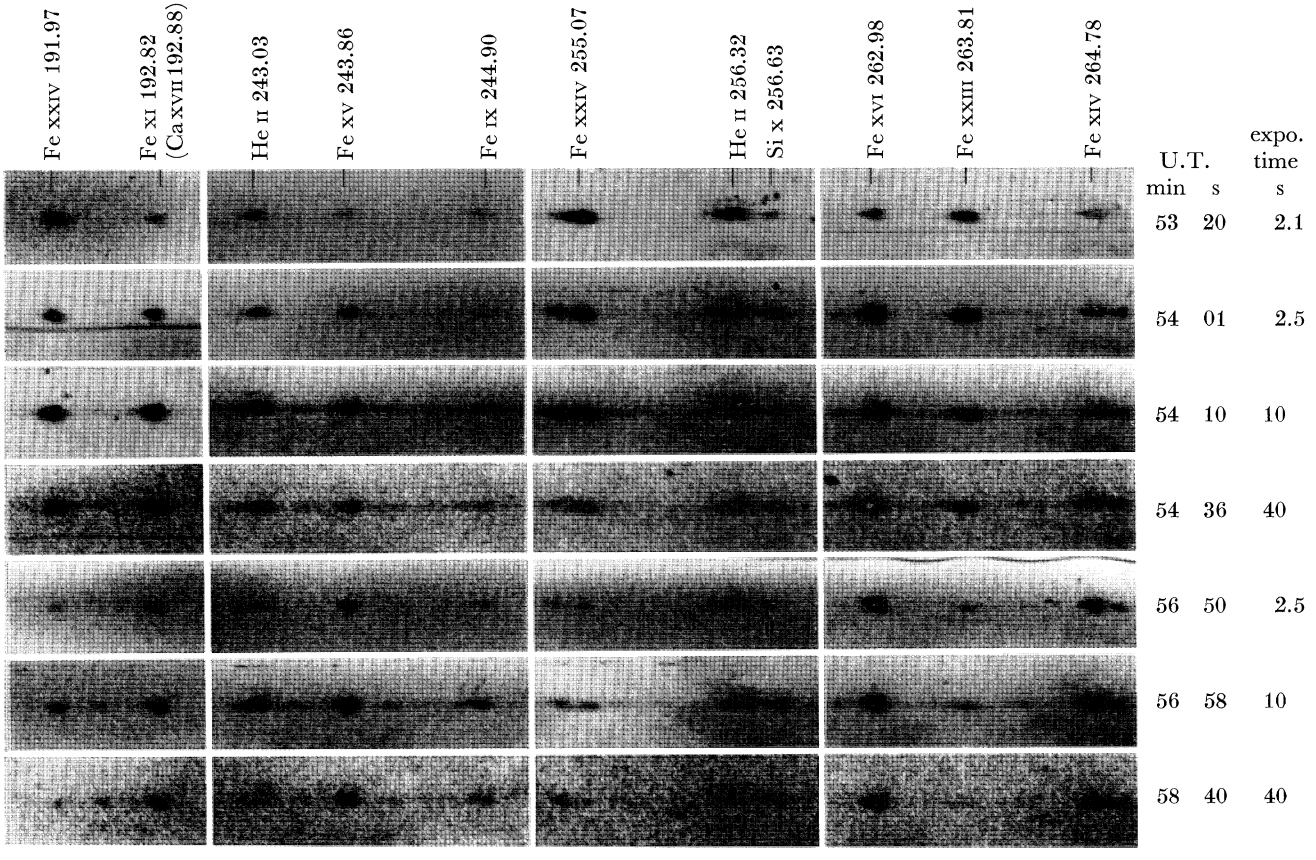

FIGURE 12. Selected portions of the 9 August 1973 subflare spectroheliograms.

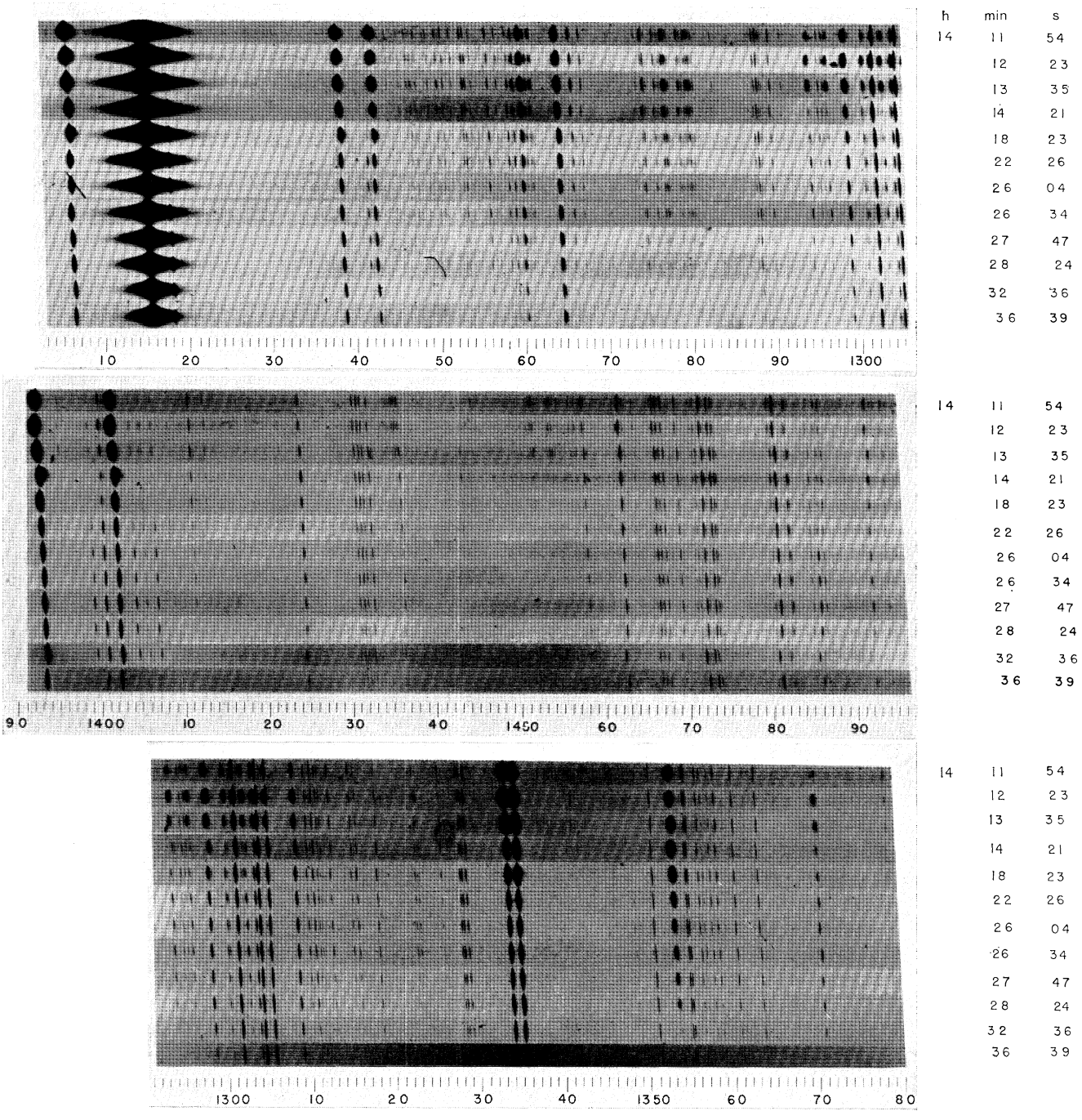

FIGURE 9. A time sequence of 15 June 1973 flare spectra, wavelength range 1200–1305 Å. The sequence begins with a spectrum, taken during the explosive phase.

FIGURE 10. A time sequence of 15 June 1973 flare spectra, wavelength range 1390–1495 Å.

FIGURE 11. A time sequence of 15 June 1973 flare spectra, wavelength range 1295–1380 Å.

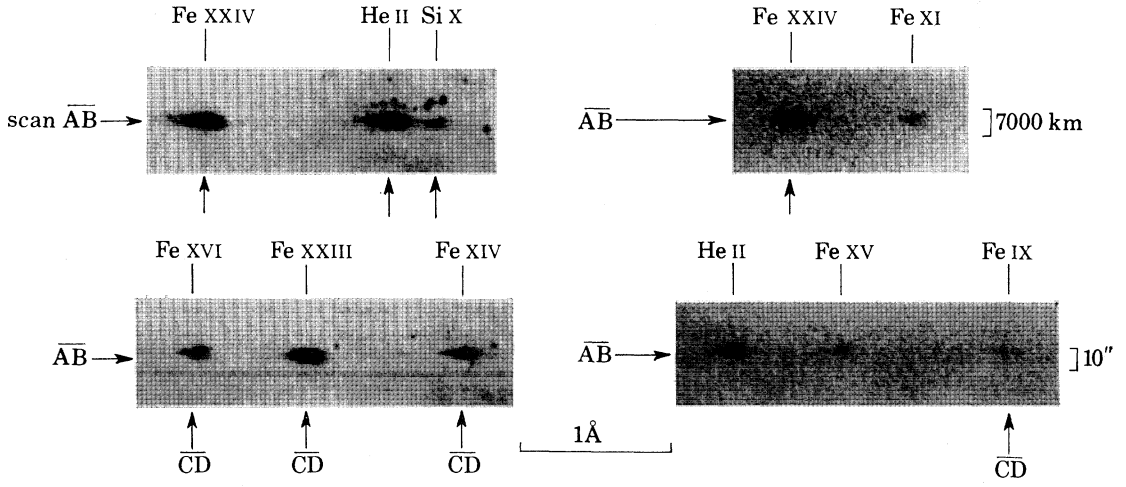

FIGURE 13. The kernel of the 9 August 1973 subflare as photographed on the first plate at 15h53min20s U.T

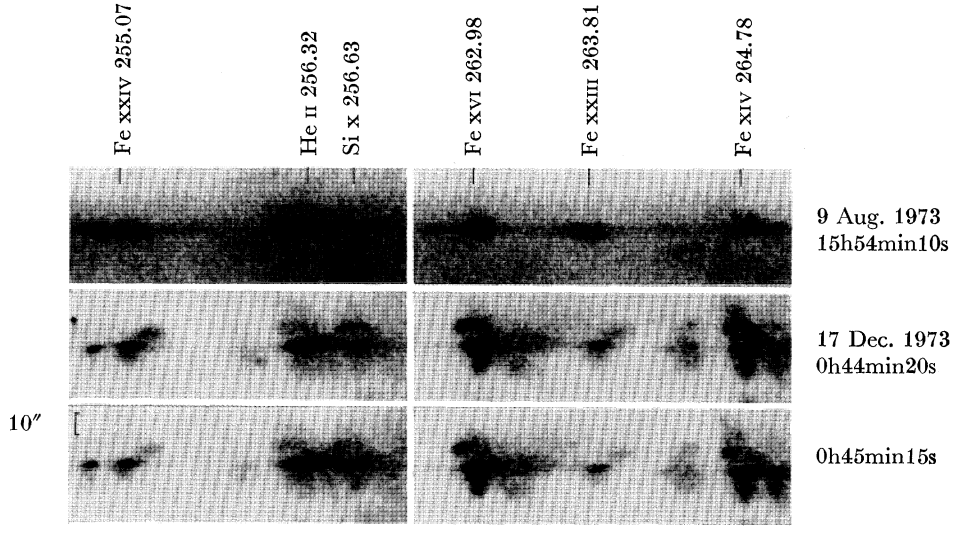

FIGURE 16. Fe XXIII 264 Å and Fe XXIV 255 Å kernels and clouds. Comparison of images of the 9 August 1973 and the 17 December 1973 events.

originating at ionization temperatures from 100 000 to 300 000 K. The spectroheliograms showed also strong line shifts and broadening in He II and coronal lines during the explosive phase. It is therefore safe to assume, that the line broadening mechanism of the transition zone lines is of the same origin like that of the cooler coronal lines during this phase of the flare. The whole region of the compact plage seems to be influenced by line broadening, as has been pointed out before. The same elongation of the plage images along the direction of dispersion can be seen, if one compares Fe XVI image at 14h11 and 14h14 (figure 3). The effect is mostly pronounced in Ne VII, see figure 4, unfortunately the Ne VII flare images are somewhat overexposed.

If the whole plage region is influenced by line broadening and shifts, a propagating mechanism must be found which influence presumably at once, the entire region. Because the compact plages are the footprints of the loops, the high energetic electrons being captured by these loops and travelling downward toward the solar surface will heat those regions preferably and cause the observed turbulence in the spectrum of the transition zone. Whether other mechanisms than turbulence contribute to the line broadening remains unanswered at this time. Spicer & Davis (1975) have pointed out recently, that plasma instabilities driven by high energetic beams can increase the micro-electric fields considerably and in this way cause Starck broadening. It will be very difficult to distinguish such a mechanism from the Doppler motions which are present in the flare plasma without doubt.

Completely different is the behaviour of all forbidden and spin-forbidden lines, which are not enhanced during the first phase, but show up strongly at the moment when the Doppler broadening of the resonance lines has stopped. A typical example are the O IV intersystem lines at 1400 Å (figure 10, plate 35) which are not enhanced during the early, explosive phase of the flare, but become strong at 14h22, when the turbulence in the transition zone lines has ceased. (The same can be said about the forbidden Fe XII line at 1241 Å.) One notices also, that these lines do not show the strong Doppler broadening and shifts of the allowed transitions. From the location of the slit above the hot Fe XXIV cloud and the most explosive portion of the flare plasma along the bridge one may conclude, that these lines represent the recombination spectrum of the transition zone and the cooling corona, at the time when the non-thermal heating has ceased and the plasma returns to thermodynamic equilibrium.

Another particular different feature in the line spectrum is the Fe XXI $^3P_1$–$^3P_0$ forbidden transition at 1354 Å (figure 11, plate 35) Brueckner 1974; Doschek *et al.* 1975). It does not show the uneven structure of the ionized resonance lines along the slit; it also peaks later (around 14h21). Because the line is formed at a temperature of approximately 10^7 K one would therefore expect it originating from the trapped, very hot flare plasma, which shows strongly during the initial phase in Fe XXIV and Fe XXIII. Turbulent motion in the Fe XXI line have been determined to be approximately 30–60 km s^{-1} which is considerably less than those motions seen in the transition zone lines at particular points of the plage.

For a complex event like the 15 June flare, it seems to be very difficult to pinpoint the location of the prime energy release, specifically because no images exist taken during the initial or flash phase of the event. In the following, arguments will be summarized for two possible models: (*a*) It is conceivable that the initial energy release occurred in the corona, manifested in the hot Fe XXIV cloud over a large volume (*ca.* 30″ diameter). High energy beams would then be guided along the loop structure above the plage region hitting the solar surface and causing the Doppler broadening at the footprints, where the diameter of the loops presumably becomes smaller than it is in the corona. It must be assumed that the erupting material seen during the explosive phase

is accelerated by secondary processes, like extreme heating of the lower denser parts of the loops. After very fast heating caused by high energy beams, the material would expand and propel upwards. When seen in the ultraviolet spectroheliograms, the fast moving material has already expanded adiabatically to temperatures as low as several million kelvins to be visible in the coronal and transition lines. Although this picture seems to be artificial, it is in agreement with the observations in general. There seems to be only one strong argument against it: At no point can any redshifts in the Fe XXIV cloud be seen, and turbulent velocities in this coronal plasma are less than elsewhere. But the fact that the first picture was taken 6 min after flare-onset, may not exclude the existence of such redshifts during the early phase. Another difficulty seems to be the observation, that the hot Fe XXIV cloud is spread over a large area, while the explosive events are taken place in a much smaller volume. It would therefore be more logical to expect a heating effect spreading out from a small volume into a larger one, not vice versa. But magnetic loops may be able to focus the high energy beams into the area, where most of the explosions occur. (*b*) One should not neglect the possibility, that the explosions as seen in high speed small clouds and the blast wave are marking the original energy source, which may be a very small kernel. Electrons and ions are ejected, as non-thermal beams and fast moving clouds, from a low lying energy source with velocities of up to 500 km s^{-1} as seen in the blast wave, which is purely blue-shifted. They are heating the corona above the plage to temperatures in excess of 2×10^7 K, causing the Fe XXIII and XXIV emission from a hot cloud hanging over the plage but trapped inside higher located magnetic structures, expanding and moving upwards with lower velocities, as described before. Most of the ejected electrons and ions are captured by the loop system above the plage and returned along the loops toward the plage surface, causing the immediate brightening of plages in the fringe areas of the active region as well as its central portion.

There is one conspicuous piece of evidence that indeed a very small and dense volume is the location of the energy release. During the cooling phase at 14h22 one recognizes two small, very bright, emitting areas which can be seen in many lines (figure 7). These two bright kernels are located where the explosive events occurred. But nothing in these observations supports the conjecture that they are the location of the prime energy release.

Both possible pictures of a flare have been outlined here in detail. In a later section when discussing other events they will be weighed against each other using observations of these other flares in order to derive a common picture of flares.

The 9 August 1973 subflare

In the following section a completely different event will be analysed. The 9 August subflare was very small in size as seen in all u.v. emission lines, although the brightness of many lines exceeded that of the 15 June event. Furthermore, during the 5 min period of the observations, the volume of the emitting plasma did not change, it rather decreased toward the end. And finally, the X u.v. pictures do not show any measurable side effects like the heating of high arches or brightening of plage areas. It is very likely to assume that the kernel itself was the location of the prime energy source and that this source had been contained. Therefore, this event is much more suitable for an investigation of the energy release mechanism than an explosive event like the 15 June flare, where the secondary effects cover very much the primary ones and line profiles become very irregular after an explosion has taken place, resulting in material moving in all directions with different velocities.

Selected lines of 7 spectroheliograms taken between 15h33 U.T. and 15h49 U.T. are

presented in figure 12, plate 34. It is evident from these pictures, that the volume occupied by the flare plasma at different temperatures seems to be the same for all lines. When judging the pictures one has to keep in mind the wide variety of intensities of different lines, which produce different densities on the plates. It is also important to note, that different exposure times of the original plates are used in the composition of this figure. Nevertheless, seen with the proper exposure, the flare kernel shows fine structure, as demonstrated in figure 13, plate 36. This fine structure seems to consist of two very small emitting regions, the lower one exhibiting much wider lines. These wide lines almost parallel to the direction of dispersion can be seen in the lower kernel in the properly exposed images of He II 243 Å and Fe XIV at 264 Å (figure 13). All other images are either over- or underexposed and therefore do not show this fine detailed structure.

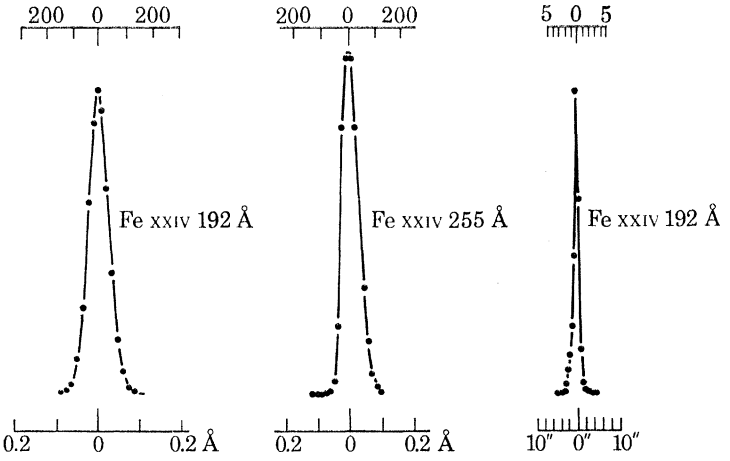

FIGURE 14. Photometric tracings of the Fe XXIV emission kernel at 192 Å and 255 Å, 9 August 1973 subflare. The left two tracings are parallel to dispersion, the right one perpendicular.

Photometric traces along the arrows marked in figure 13, have been made parallel and perpendicular to the dispersion. An example of the Fe XXIV tracings is given in figure 14. At first glance it is evident that the full width at half maximum of the trace perpendicular to the dispersion ($\simeq$ 2.0″) is much narrower than the full width at half maximum along the direction of dispersion (0.062 Å $\hat{\simeq}$ 4.7″). This alone is a strong argument, that the image broadening along the axis of dispersion is caused by a wavelength broadening of the lines, especially if one considers the fact, that the small, streak-like lines are elongated along the direction of dispersion. But by accident an extended spatial structure could be located along the axis of dispersion. Therefore, the scanned profile along the direction of dispersion of the Fe XXIV lines at 192 Å and 256 Å line which originate from the same multiplet are compared in figure 14. The linear (wavelength) scale of the 192 Å line has been expanded by a factor of 256/192 = 1.32 to demonstrate that the Doppler half width $\Delta\lambda/\lambda$ of the 192 Å line is approximately the same as that of the 255 Å line, namely 0.062 Å. This is the strongest evidence for wavelength rather than image broadening of the lines which can be presented. If a spatial structure along the direction of dispersion would exist which is larger than the Doppler broadening of the line, a wavelength dependence of the half width should not be observed. It is therefore plausible to assume that the size of the source, in the direction of dispersion is the same as measured perpendicular to the dispersion. This assumption allows one to disregard the spatial extent of the source parallel to the direction of dispersion, because it is small compared with the line broadening.

Absolute values for the line width as they have been quoted, are very difficult to determine in these very small, sometimes overexposed images, because of grain noise and uncertainties of the characteristic curves of the film. Therefore, an error margin of a factor of two for the line width has been estimated, which results in lower and upper limits for the line width, as shown in table 2. But the line width listed in this table are the mean values of at least six plates scanned for each line, reducing random errors but neglecting the time development of these profiles. Therefore the remaining error is of systematic nature, if the half width of a selected profile must be changed by a certain factor, this factor must be applied to all other profiles. The result which can be seen in table 2 is the fact that all line width for ions of different excitation temperatures are the same within error limits, indicating nonthermal motions of considerable magnitude. These ion velocities of 60–120 km s^{-1} are confined into the small volume for which only an upper limit of 2.0 arc $sec^3 \triangleq (1400\,km)^3$ can be given. In reality, this volume may be smaller. The coexistence of ions formed at excitation temperature from 10^6 to 2×10^7 K indicates strong electron temperature gradients confined in this small volume.

TABLE 2. FLARE 9 AUGUST 1973, EMISSION LINE PROFILES

ion	Fe XXIV	Fe XXIV	Fe XXIII	Fe XVI	Fe XIV	Si X	Fe IX (?)	He II
wavelength/Å	192	255	264	263	265	256	243	256
fullwidth at half maximum/km s^{-1}								
maximum	204	189	181	168	177	168	228	276
minimum	97	86	94	95	105	104	98	158
Doppler width/km s^{-1}								
maximum	123	114	109	101	106	101	137	166
minimum	58	52	56	57	63	62	59	95
$T_{kin}/10^6$ K								
maximum	50	38	35	35	39	19	60	7
minimum	11	9	11	11	13	7	12	2
$T_e/10^6$ K	20	20	16	3.1	2	1.6	0.7	(?)†

† The electron temperatures in table 2 have been taken from Jordan (1969, 1970).

In figure 15, the time behaviour of the accompanying X-ray radiation as seen from Solrad 9 has been plotted, together with the time dependence of the line emission of the different ions. In addition, a temperature and emission measure as outlined by Dere, Horan & Kreplin (1974) has been calculated and plotted. It is questionable, whether the assumptions made for the X-ray emission measure calculations are valid for a turbulent plasma as seen in the small volume. But the lower values of the ion temperatures as determined from the line profiles indicate an ion temperature of 11×10^6 K (see table 2), which seems to be in agreement with the temperatures calculated from the X-ray emission.

Accepting the calculated emission measure values, one obtains a minimum density of 3×10^{12} for the 11×10^6 K plasma. The total X-ray emission from the flare as seen from Solrad 9 amounts to 3×10^{21} J, measured in the 8–16 Å channel. (The contribution from the higher energy channels are negligible.) The total kinetic energy in the 11×10^6 K plasma as seen at a particular moment is 8×10^{20} J, which indicates, that the energy release took place in a very short time interval, assuming that energy losses other than radiation can be neglected. Whether this is true cannot be proven other than by the observation, that the event was confined always to the same small volume. One notices in figure 15, that the time change of the Fe XXIV emission seems to be well correlated to the 0.5–3 Å X-ray radiation.

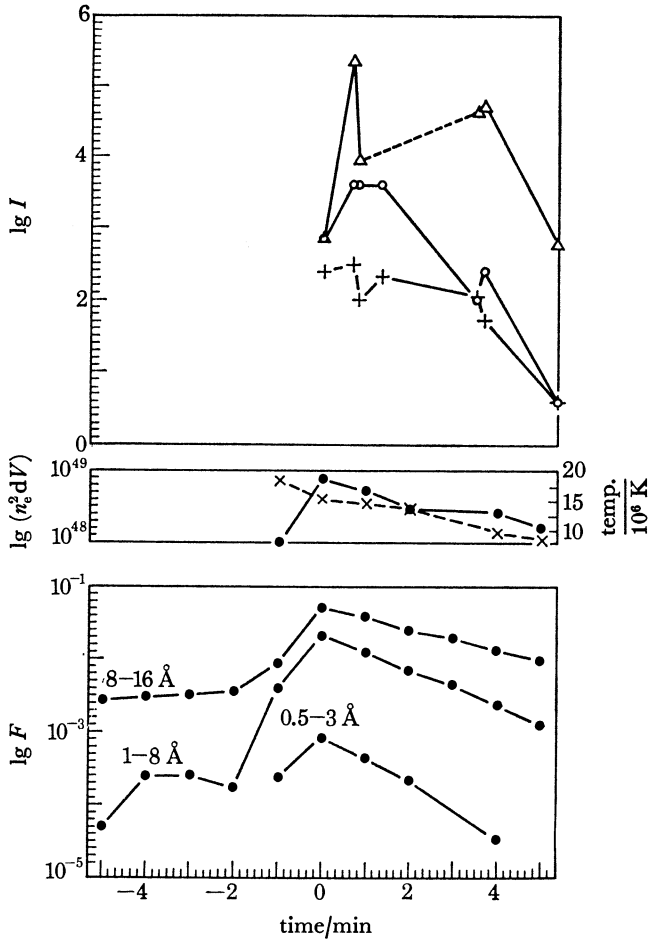

FIGURE 15. Upper part: Intensity of the 9 August 1973 subflare kernel against time as seen in Fe XXIV 192 Å (○), Fe XVI, 263 Å (△) and Fe IX (?), 243 Å (+); intensity in relative units. Middle part: X-ray emission measure (●) and temperature (×). Lower part: X-ray flux (0.5–3 Å) (1–8 Å) (8–16 Å) channels Solrad 9 against time. Zero time is 15h53min20.6s U.T.

Further evidence for the dual appearance of the Fe XXIII and Fe XXIV emission

As said before, the 9 August event does not show the coronal hot cloud as seen in the 15 June flare. The very hot plasma is confined in a very small volume. It is impossible to determine the height of the emission above the Sun's surface. There is only an indication, that the Fe XXIII and Fe XXIV emission is separated spatially from the emission of the lower ions (see figure 13). In the following, a comparison will be made between the appearance of Fe XXIII and Fe XXIV in the 9 August event and another flare, which was photographed on 17 December 1973. Although the latter event was complex in its nature, a second explosion occurred while the flare was in progress. Figure 16, plate 36, shows the comparison. While the hot emission in the 9 August event (upper row of images) was confined in a sharp streak, elongated along the direction of dispersion, it has a dual appearance in the 17 December flare at 0h 44 min 20s. Besides the fact, that there are two spatially separated emission centres, the lower one seems to consist of two features: a sharp, point-like source elongated along the dispersion, accompanied by a cloudy halo surrounding it One has the impression of a very dense hot kernel surrounded by an extended cloud of less density. One minute later at 0h45min15s the cloud has shrunk considerably while the kernel is still very bright in Fe XXIII and Fe XXIV.

Figure 17, plate 37, shows another small flare, photographed on 5 September 1973. The hot plasma is clearly separated from images of lower ionization stages. Fe XXIII and Fe XXIV clouds are located with their maximum emission marked by an arrow *B*, seemingly above the He II plage, which extends from *A* to *C*. Elongated emission features in He II, Fe XVI and Fe XIV can be seen along the dispersion marked by *C*. Fe XVI shows another feature, tilted 30° from the direction of dispersion. If one interprets the Fe XXIV emission as a loop, bridging the He II plage, then the tilted Fe XVI feature may be its extension down to the surface. Assuming that the streak like features in He II, Fe XVI and Fe XIV along *C* are located at the footprint of this loop, they are red shifted and indicate therefore material streaming into the solar surface with a velocity of approximately 200 km s^{-1}. In this picture, the hot plasma would be located somewhere along the imaginary loop. Six minutes later the Fe XXIII and Fe XXIV emission has disappeared and a loop connecting *A* and *C* is now emitting strongly in the cooler ions Ca XVII (Fe XI) at 192.82 Å, Si X, Fe XVI, and Fe XIV. The appearance of the post-flare loop at the very location, where the Fe XXIII and Fe XXIV emission was seen, suggests that the hot plasma was located along this loop and during the cooling period of the originally very hot plasma, heat is transferred into the loop which is subsequently cooling by conduction to the surface, making it visible in many cooler ionization stages. The sharp Fe XXIII kernel as seen in the 9 August and 17 December events is missing here. But one has to keep in mind, that only two photographs exist, none of them covering the initial phase of the flare.

The images of the 5 September event as shown in figure 17 are very suggestive to place the primary energy source into a loop arching an active region. But one must be very careful, before definite statements can be made, because first of all only two spectroheliograms exist, the second one taken during the cooling phase when post-flare loops develop, which does not mean that such a structure already existed during the pre-flare condition. Secondly, we do not have any reliable information about the altitude of the hot cloud visible in Fe XXIII and Fe XXIV. But the pictures indeed seem to suggest that the Fe XXIII and Fe XXIV emission follows the later appearing cooler post-flare loop.

The 21 *January* 1974 *flare*

This flare is the only event covered completely by photographs of the N.R.L. spectroheliograph from the very beginning of a flare. A selection of the spectroheliograms in the wavelength region 237–265 Å are shown in figure 18, plate 38.

At the very beginning of the event one notices strong, Doppler broadened emission features, elongated along the dispersion in He II along the direction marked by the arrows *A* and *B*, connected by a loop, which can be seen clearly in He II 237 Å and He II 243 Å (the loop is also visible in He II 256 Å but overexposed and not clearly distinguished against the plage background). Along the direction *B* one recognizes a strong, point-like emission centre in Fe XXIV and Fe XXIII, while the emission in the coronal ions of Fe XIII through XVI is relatively weak. It is also obvious, that Fe XXIII as well as Fe XXIV are apparently shifted to the red approximately 0.1 Å from their rest wavelength, which in this case is defined assuming that the He II emission kernels are at their rest wavelength. One can interpret this shift spatially or spectrally, more precise measurements are necessary to decide between the two possibilities. Therefore, the Fe XXIII and Fe XXIV emission kernel may be detached from the He II footprint at *B*, but on the other hand, it is suspicious, that the hot kernel is lined up exactly along the direction of dispersion with the He II emission. If interpreted as a Doppler shift, the sharpness of the emission in Fe XXIII and Fe XXIV is remarkable, one would expect a considerable smearing effect during the 20 s long exposure, because the

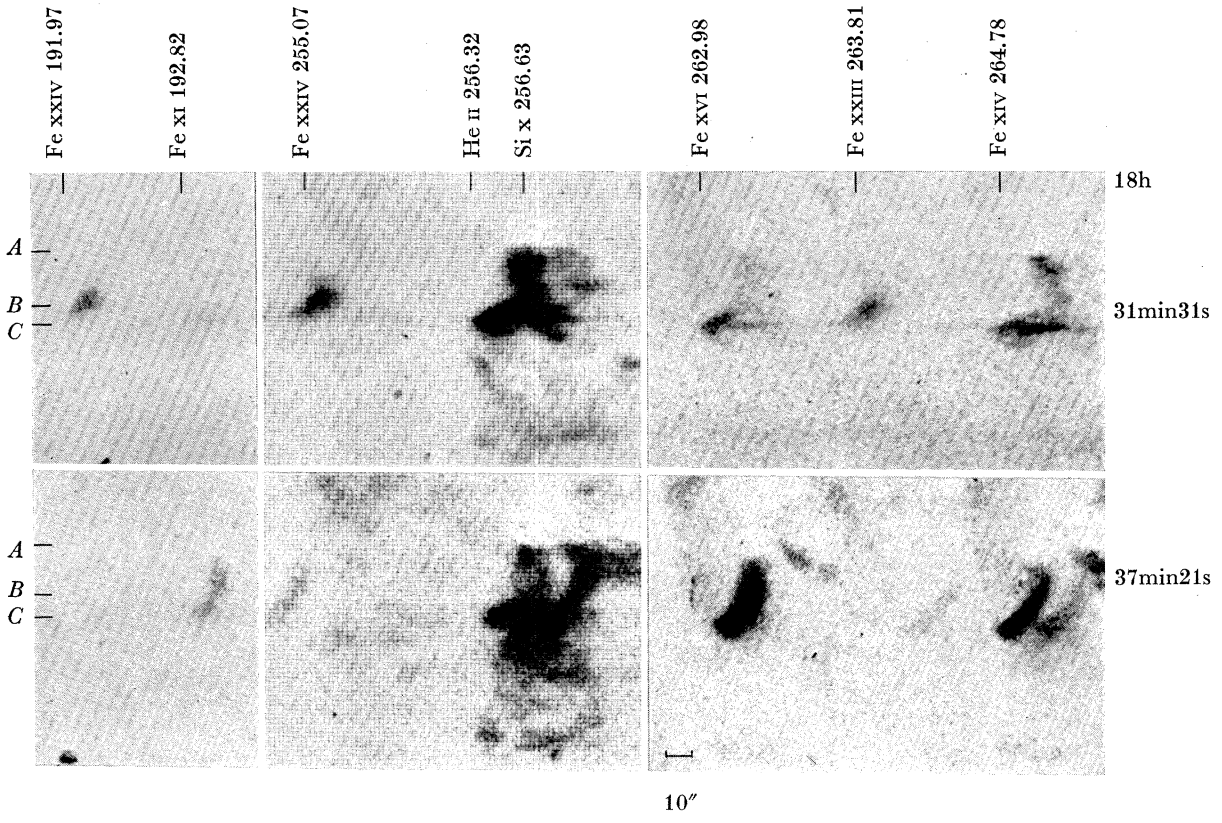

FIGURE 17. Fe XXIII 264 Å, Fe XXIV 192 Å and 255 Å clouds compared with post flare loops in Fe XVI 263 Å and Fe XIV 265 Å as seen in two plates, photographed during a small disk flare on 5 September 1973.

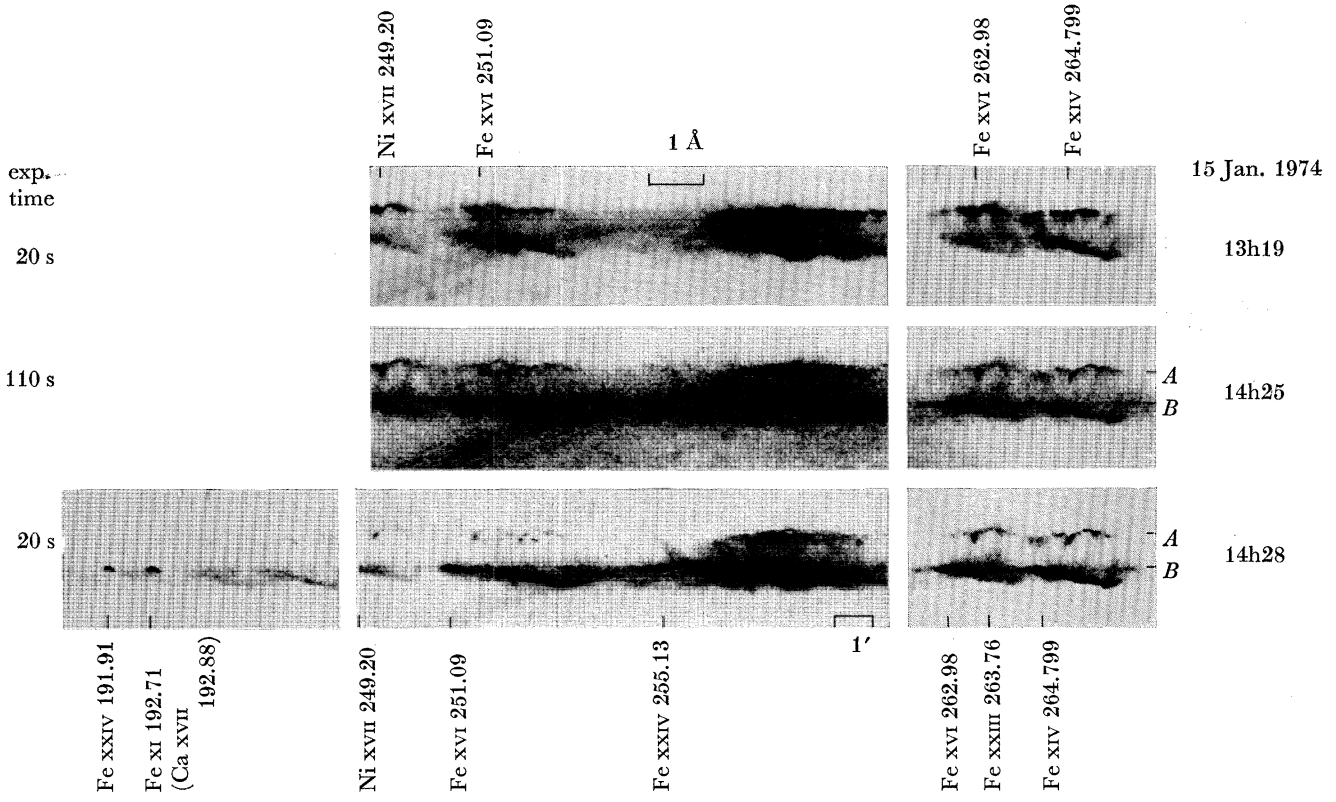

FIGURE 21. Loops, plages and a flare kernel at the limb, 15 January 1974.

(*Facing p.* 454)

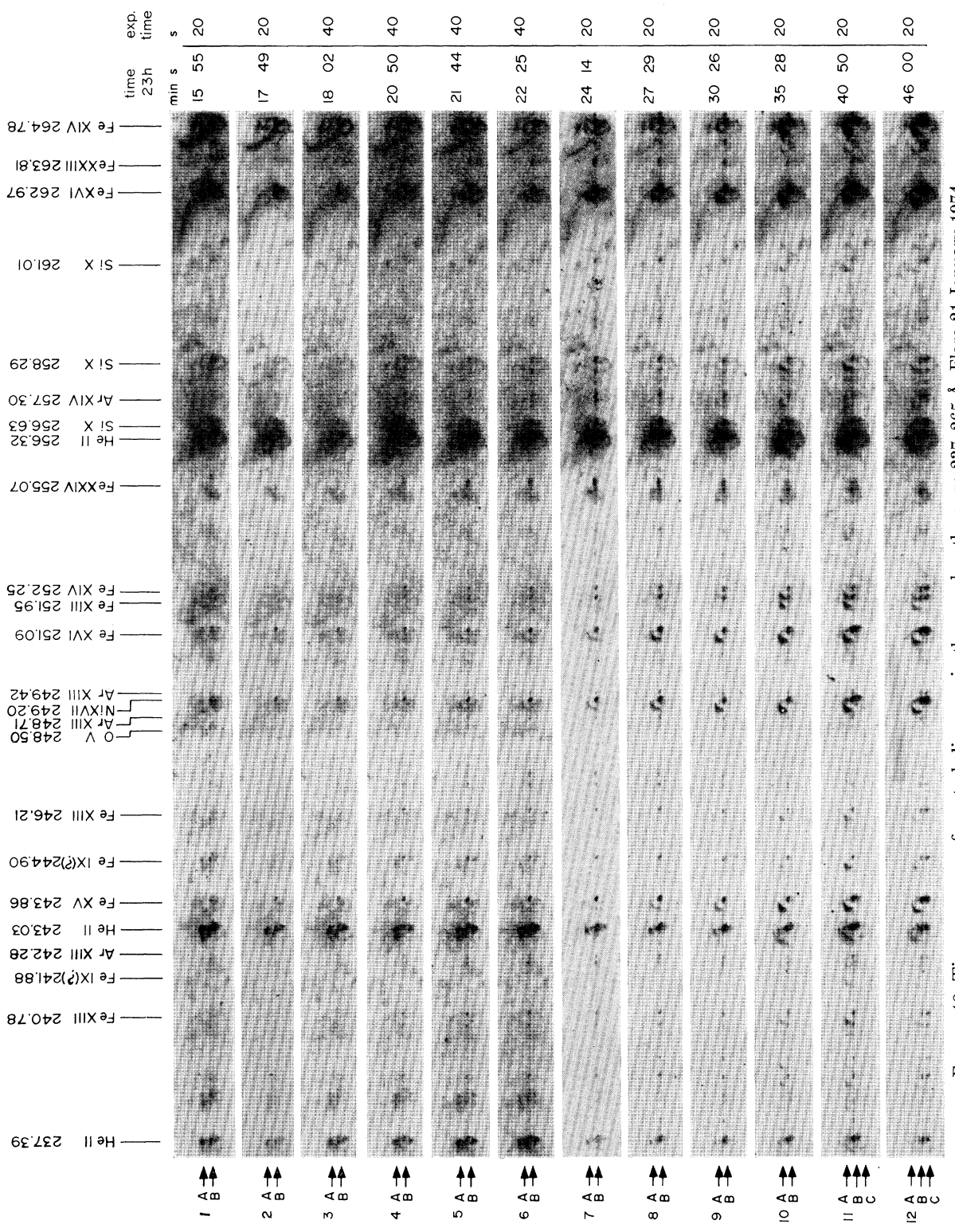

FIGURE 18. Time sequence of spectroheliograms in the wavelength range 237–265 Å. Flare 21 January 1974.

velocity corresponding to this shift would be 120 km s^{-1}. But it is possible, that a movement almost exactly along the line of sight took place, which would not result in any smearing of the image. Another feature close to the rest wavelength of Fe XXIV is a cloud, centred around the emission kernel, extending perpendicular to the direction of dispersion located to the blue from the Fe XXIV emission rest wavelength. Its origin is highly questionable.

Following the time sequence one recognizes the sudden disappearance of the Fe XXIII and Fe XXIV kernel in exposure 2, taken 2 min later, but the kernel reappears this time located at its rest wavelength beginning with exposure 4, reaches its maximum brightness at exposure 7, to fade out slowly toward the end of the sequence. While the kernel is weak in Fe XVI (251 Å) and Ni XVII (249.2 Å) during the first exposure it gradually becomes more intense in these lines, which peak around exposure 8 when the hotter lines are already decreasing in intensity. Also the cooler lines, like Fe XIII (251.95 Å) are very weak during the first six exposures to peak around exposure 10. (All of these remarks apply to the flare kernel located at *B*.)

The sudden disappearance of the kernel in Fe XXIII and Fe XXIV on exposure 2 and its reappearance later can be interpreted in two different ways: (*a*) An initial catastrophic energy release heats the small volume to temperatures in the 20×10^6 K region where Fe XXIII and Fe XXIV emit, followed by a rapid cooling. Subsequently a new, but slower energy buildup heats the kernel once

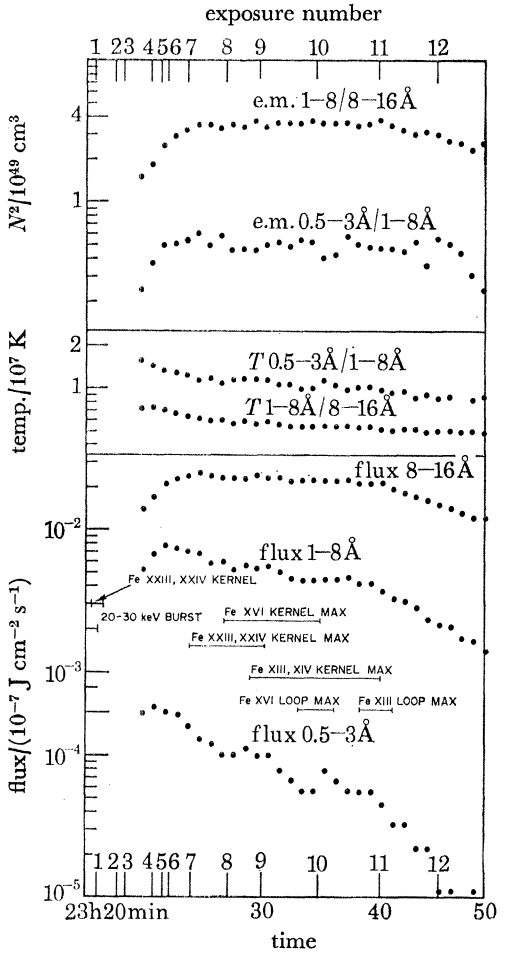

FIGURE 19. X-ray fluxes, emission measure and temperatures, Solrad 9, 21 January 1974 flare.

more, until ions like Fe XXIII and XXIV can exist. (*b*) The Fe XXIII and Fe XXIV images in exposure 1 represent the temperature of the kernel at this time, which is subsequently heated up to much higher temperatures around 10^8 K, where Fe XXIII and Fe XXIV disappear, and the reappearance on later exposures reflects the cooling flare kernel at that time, when temperatures drop from 10^8 K down to 2×10^7 K.

In order to decide between these two possibilities, it is necessary to compare the spectroheliograms with the X-ray emission, as recorded by Solrad 9 and plotted in figure 19. Unfortunately, the Solrad 9 measurements do not cover the very first phase of the flare, but it is evident, that the 0.5–3 flux peaks between exposures 3 and 4 at a time when the Fe XXIV emission is still weak, after its initial appearance on exposure 1. Therefore, a source must exist at this time, which emits the X-rays in the 0.5–3 Å channel, but is not visible in Fe XXIII and Fe XXIV. From this it seems to be evident, that this source has a temperature high enough to ionize Fe to even higher ionization stages than Fe XXIII and Fe XXIV, which disappear around 50×10^6 K. The other explanation, where an initial energy release is followed by another build-up seems to be inconceivable with the 0.5–3 Å X-ray flux. This does not exclude the possibility that energy is still produced during the later stage, but at lower temperatures.

It seems now doubtful, whether the temperature and emission measure calculation from the X-ray flux as plotted in figure 19 are valid, because the temperature calculated from the 0.5–3 Å and 1–8 Å channels drops down to 10×10^6 K around exposure 7 when the Fe XXIV emission reaches its peak. It is likely, that a more differentiated temperature analysis, which takes into account a multithermal origin of the X-ray emission can satisfy the observation better. But this cannot be done from three X-ray channels only.

In figure 20 the correlation of the Fe XXIV emission at 255 Å on exposure 1 with a hard X-ray burst, as seen from OSO-7 by the X-ray spectrometer of the University of California, San Diego is shown. Exposure 1 was taken, while the burst was still in progress, exposure 2, which does not show the Fe XXIV emission, was taken at a time when the 20–30 keV burst had clearly ceased. But at the same time, the 5.1–6.6 keV X-rays intensity is still rising. Unfortunately, the satellite went into darkness at 23h17min20s. The correlation of the hard X-ray burst with the appearance of the Fe XXIV kernel on exposure 1 may reflect the transitionary stage of the plasma when it is heated up to extreme high temperatures by non-thermal processes. The cooling phase of the flare is characterized by strong emission in the flare kernel at *B* (figure 18) in lower ionization stages. A strong loop develops, connecting *A* with *B*, but seemingly detached from the flare kernel. This loop seems to expand and move away from the kernel. A second kernel appears on exposure 11 along the direction marked by *C*. It can be seen first in Fe XVI and Ni XVII, later on exposure 12 also in lower ionization stages, like Fe XIII. (It does not appear in Fe XXIV. There appears another, lower temperature line shortward of 255.0 Å, which must not be mistaken with the Fe XXIV line. The concurrent absence of the Fe XXIII line at 263.81 Å in this feature at *C* proves this point.)

Flare loops at the limb

On 15 January 1974, a series of 3 spectroheliograms were taken, which show a small flare in progress at the limb, portions of these spectroheliograms are reproduced in figure 21. At 13h29 one recognizes a typical loop formation above a plage at the limb. The top of the loops show the familiar bright 'knot' structure, spatially sharper in Fe XIV than in Fe XVI. The upper wavelength scale in figure 21, plate 37, has been adjusted for one particularly bright 'knot' at the top of these loops as marked by *A*. A flare kernel can be seen in the two following images marked *B*

(lower wavelength scale) taken at 14h25 and 14h28. It is distinguished from the loop system by the appearance of the Fe XXIV and Fe XXIII emission at 192 Å, 255 Å, and 264 Å and seems to be located very close to the surface. The loop structure has distinctly changed. But there seems to be no connection between the loops at higher altitudes and the low lying flare kernel. One may interpret the blurred feature above the Fe XXIII line as a hot coronal cloud extending toward the tops of the loops, but this can be a misidentification with overlapping images of the loop structure itself. Nevertheless, this picture seems to confirm the earlier speculation of a very hot small flare kernel at low altitudes surrounded by a hot cloud of coronal gas above it, which is heated from the kernel.

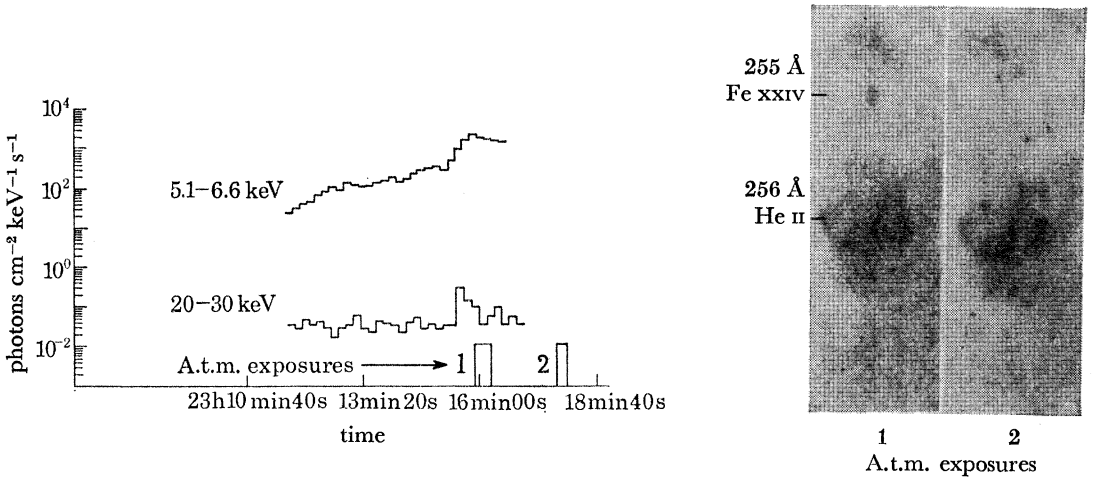

FIGURE 20. Correlation of the 20–30 keV X-ray burst (University of California, OSO-7 X-ray spectrometer) with Fe XXIV 255 Å images.

Summary and conclusions

It is evident, that the energy release in small flares is confined to a very small volume, the hot flare kernel, which has smaller dimensions than the resolution of the telescope (< 1400 km). Ion temperatures in these kernels seem to exceed 20×10^6 K. As secondary effect one observes a cloud of heated coronal gas above these kernels at 20×10^6 K. It is difficult to distinguish, whether in the latter cases energy production takes place in the larger coronal volume, but a plausible assumption would be that this is not the case, rather the surrounding corona is heated from the kernel. There is a clear correlation between the appearance of this coronal cloud and the brightness of the kernel. It seems to be the case, that strong coronal heating takes place, when the kernel is not confined but is exploding after being heated to very high temperatures. These temperatures in the hot flare kernel may exceed those measurable by the emission of Fe XXIII and Fe XXIV, as it seems to be the case in the 15 January event. Neupert (1971 *b*) has reported the appearance of Fe XXV and Fe XXVI lines during the early phase of a flare. If these lines are emitted from the same volume, where we can see Fe XXIV emission, the picture of a very hot flare kernel would be supported substantially. Although Neupert's instrument did not have spatial resolution, it is a plausible assumption, that the Fe XXV and Fe XXVI plasma ($T > 10^8$ K) is emitted from the same volume, where Fe XXIV originates. While the observations are clear in the cases of smaller events, they cannot confirm with certainty a similar picture for the large events like the 15 June flare. There is evidence, that the initial energy release even in such an event takes place also in a small volume close to the surface. All other effects of a flare – the heating of the corona above the

explosive site, the trapping of the high temperature coronal gas below the high lying loop structures and the subsequent conduction of these particles along the loop downward to the surface with the accompanying brightening of the plages must be considered to be of secondary nature.

The basic argument, which remains to be settled is whether the prime energy release of a flare occurs in the high temperature coronal cloud or in the small, very hot and dense flare kernel. The observations seem to support the latter case, because in no instance has there been seen strong streams of hot coronal gas downward, either manifested by movements or Doppler-shifts. But it could be also argued that the hot coronal cloud is at the same time imbetting streams of high energy particles. These must definitely be invoked to explain the strong Doppler motions at the footprints of the loops in the brightened plages. On the other hand, they must not necessarily originate in the corona. The observed blast wave and ejecta moving outward in the 15 June event may indicate that they are coming from lower layers, although in this case a definite altitude of their origin can not be determined.

If one takes the position that the small flare kernels are the origin of the prime energy release then a basic difficulty arises about the question of mass and energy supply. It has been shown in this paper, that this difficulty does not exist for the small subflares, where densities of about $3 \times 10^{12}\,\mathrm{cm}^{-3}$ and total energies of 10^{22} J are within the framework of conventional flare theories. But this would not be the case any more for large events, which require at least 10^{24} J and 10^{41} particles to account for their X-ray emission. It has been argued, that one must find traces of these events in the change of photospheric and chromospheric structures, if the mass is supplied from these regions. On the other hand, the observations of the flare kernels' size are still determined by the resolution of the instrument (*ca.* 2.0″). The true size of the flare kernels can be therefore even much smaller. One could speculate that the flare kernels represent nothing else but a very thin channel, through which high energy particles are ejected into the corona, originating from much deeper layers, perhaps even below the photosphere. If they have a size smaller than a granule, one would not detect them in visible light pictures. Perhaps the white light kernels occasionally observed in very energetic flares (McIntosh 1972), are the photospheric manifestation of the observed u.v. kernels.

It is a pleasure to name first of all the members of the three Skylab crews, C. Conrad, Dr J. Kerwin, P. Weitz, A. Bean, Dr O. Garriott, J. Lousma, G. Carr, Dr E. Gibson, and W. Pogue who observed with magnificent skill all the flares mentioned in this analysis. Their observing techniques, which they refined during the emission succeeded finally in the series of plates, covering the 21 January flare from the very beginning taken by Dr E. Gibson. I have to thank Mr M. Van Hoosier for his patient efforts in photographic photometry to derive the line profiles of the 9 August flare. Dr K. Dere prepared the Solrad-9 X-ray plots. I am grateful to Dr D. Datlowe for communicating the X-ray measurements of the University of California, San Diego. Helpful discussion with Drs Cheng, Tousey, and Widing, as well as with Mr O. Moe and D. Spicer contributed to this paper. Mr S. Delaney prepared with great skill the numerous photographic reproductions.

This work was supported by N.A.S.A. DPR S-60404G.

References (Brueckner)

Bartoe, J.-D. F., Brueckner, G. E., Purcell, J. D. & Tousey, R. 1974 *Proc. Soc. Photo-Opt. Instr. Eng.* **44**, 153.

Brueckner, G. E. 1974 Proceeding IAU-COSPAR Symposium No. 68, Buenos Aires, Argentina, June 1974.

Bruzek, A. 1962 *Z. Astrophys.* **54**, 225.

Dere, K. P., Horan, D. M. & Kreplin, R. W. 1974 *J. Atm. Terrestrial Phys.* **36**, 989.

Doschek, G. A., Feldman, U., Dere, K. P., Sandlin, G. D., VanHoosier, M. E., Brueckner, G. E., Purcell, J. D. & Tousey, R. 1975 *Astrophys. J. Lett.* **196**, L83.

Firth, J. G., Freeman, F. F., Gabriel, A. H., Jones, B. B., Jordan, C., Negus, C. R., Shenton, D. B. & Turner, R. F. 1974 *Mon. Not. R. astr. Soc.* **166**, 543.

Jordan, C. 1969 *Mon. Not. R. astr. Soc.* **142**, 501.

Jordan, C. 1970 *Mon. Not. R. astr. Soc.* **148**, 17.

Kononov, E. Ya., Koshelev, K. N. & Podobedova, L. I. 1974 *Opt. Spektrosk.* **37**, 3.

McIntosh, P. S. & Donnelly, R. F. 1972 *Solar Phys.* **23**, 444.

Neupert, W. M. 1971*a* *Phil. Trans. R. Soc. Lond.* A **270**, 143.

Neupert, W. M. 1971*b* In *Physics of the solar corona* (ed. C. J. Macris), p. 237. Dordrecht, Holland: D. Reidel Publishing Co.

Purcell, J. D. & Widing, K. G. 1972 *Astrophys. J.* **176**, 239.

Sandlin, G. D., Brueckner, G. E., Scherrer, V. E. & Tousey, R. 1975 (Submitted to *Astrophys. J. Lett.*)

Sheeley, N. R., Jr., Bohlin, J. D., Brueckner, G. E., Purcell, J. D., Scherrer, V. E. & Tousey, R. 1975 *Solar Phys.* **40**, 103.

Spicer, D. S. & Davis, J. 1975 *Solar Phys.* **43**, 107.

Tousey, R. 1971 *Phil. Trans. R. Soc. Lond.* A **270**, 59.

Widing, K. G., Sandlin, G. D. & Cowan, R. D. 1971 *Astrophys. J.* **169**, 405.

Widing, K. G. 1975 *Astrophys. J. Lett.* **197**, L33.

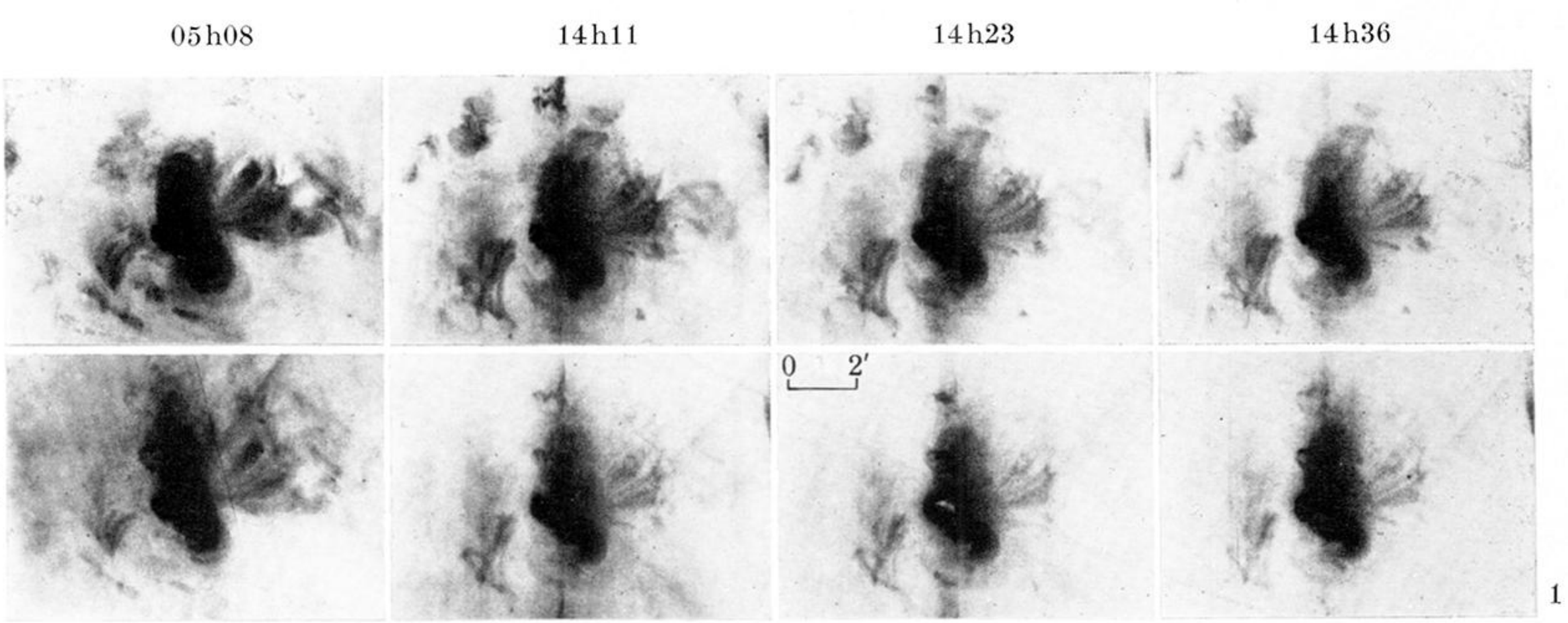

FIGURE 1. Development of the active region, in which the 15 June 1973 flare occurred as seen in Fe xv 284 Å and Fe xvi 335 Å.

FIGURE 2. The central plage and loop system before, during and after the 15 June 1973 flare; Fe xv 284 Å and Fe xvi 335 Å.

13h 52 | 14h 11 min | 14 min | 22 min | 33 min | 36 min

10^3 km/s

Fe xv 284 Å

60″

1 Å

Fe xvi 335 Å

3

Mg ix 368 Å

60″

Ne vii 465 Å

4

05h06 | 12h18 | 14h12min | 19 min | 27 min | 34 min

14h11min39s | 14h14min28s

A
B
C
D

1 Å

6

1′

FIGURES 3, 4 AND 6. For description see opposite

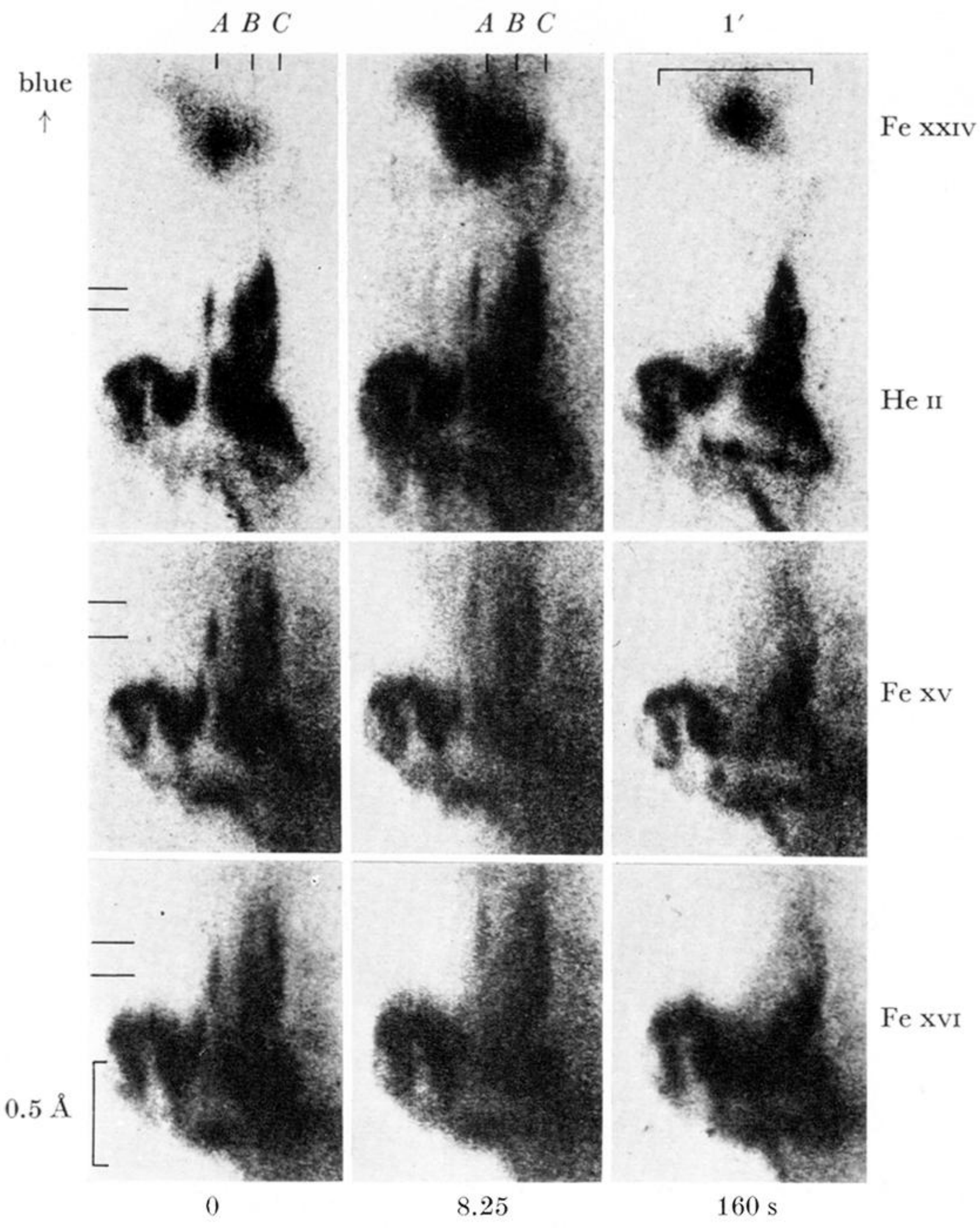

FIGURE 5. Rapid changes of 15 June 1973 flare images in Fe XV 284 Å, Fe XVI 335 Å, He II 256 Å and Fe XXIV 255 Å. Zero seconds corresponds to the time, when the first flare spectroheliogram was taken. At 160 s the explosive phase of the flare has ceased. (The images at 0 s and 160 s are 2.5 s exposure, the images at 8.25 s 10 s exposures.) The parallel lines on the left hand photos indicate Δl.

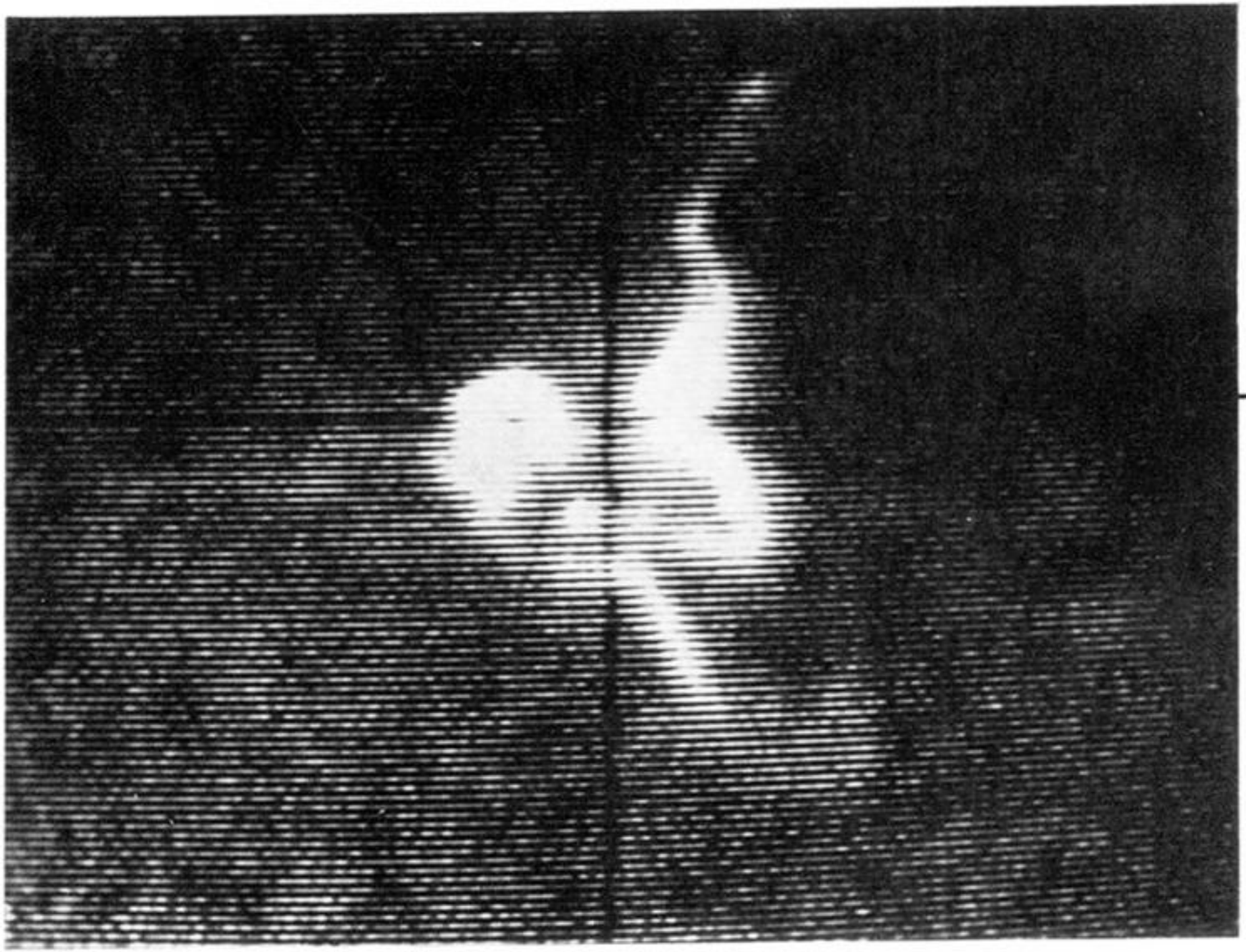

FIGURE 8. Position of the spectrograph slit on the 15 June 1973 flare Hα image. The slit was located along the vertical cross-hair.

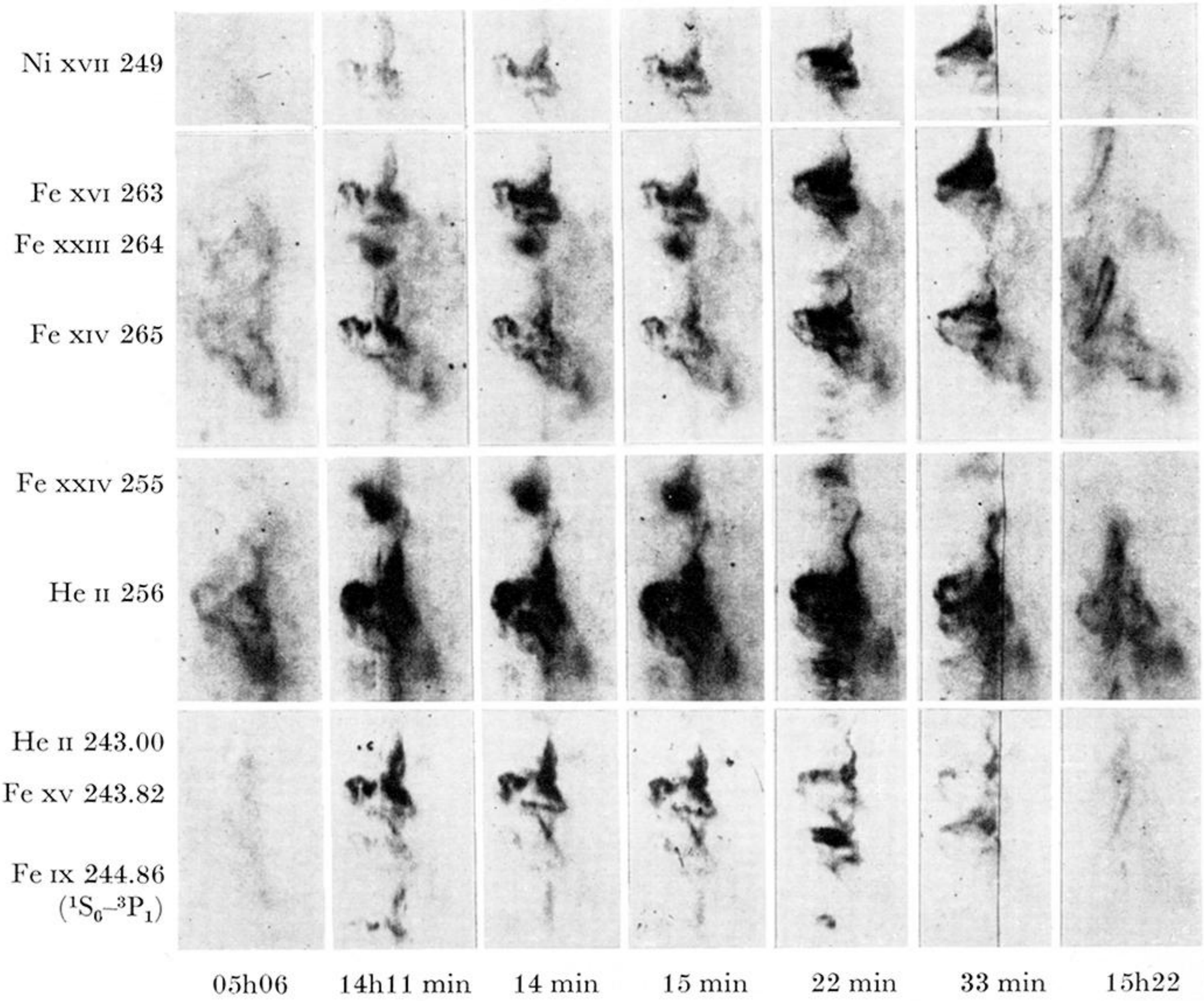

FIGURE 7. Time sequences of 15 June 1973 flare images in Ni xvii 249 Å, Fe xvi 263 Å, Fe xxiii 264 Å, Fe xiv 265 Å, Fe xxiv 255 Å, He ii 256 Å, He ii 243 Å, Fe xv 243.82 Å and Fe ix (?) 244.86 Å.

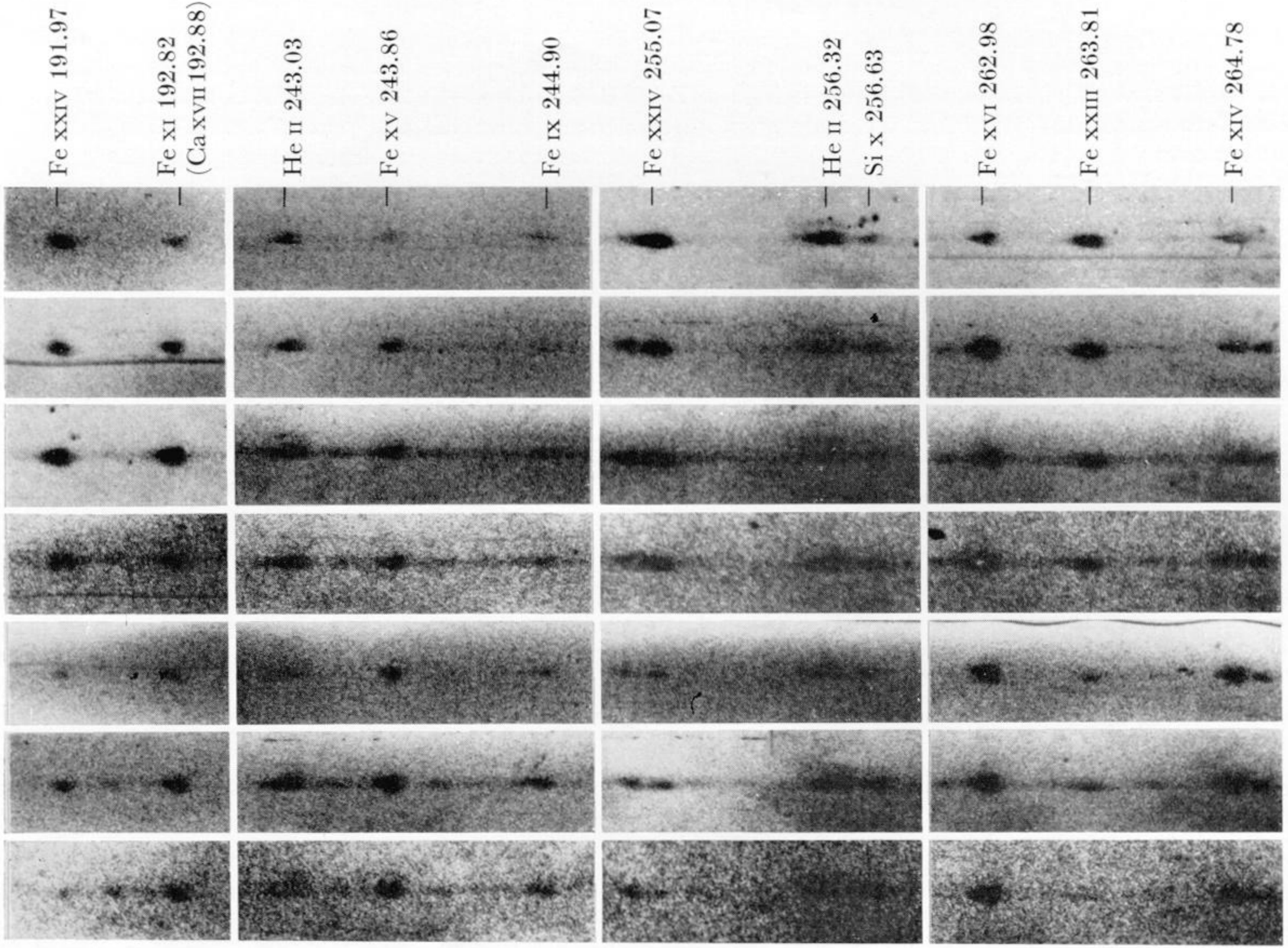

FIGURE 12. Selected portions of the 9 August 1973 subflare spectroheliograms.

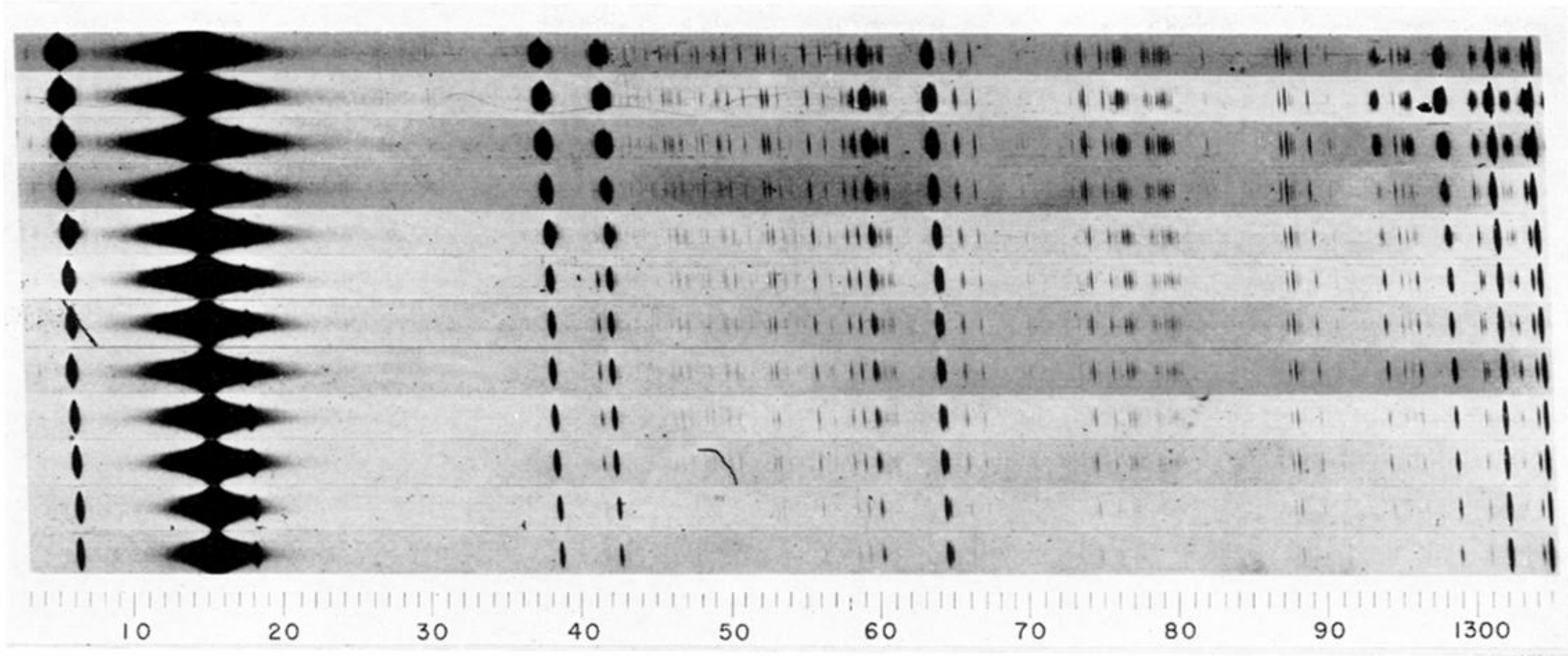

h	min	s
14	11	54
	12	23
	13	35
	14	21
	18	23
	22	26
	26	04
	26	34
	27	47
	28	24
	32	36
	36	39

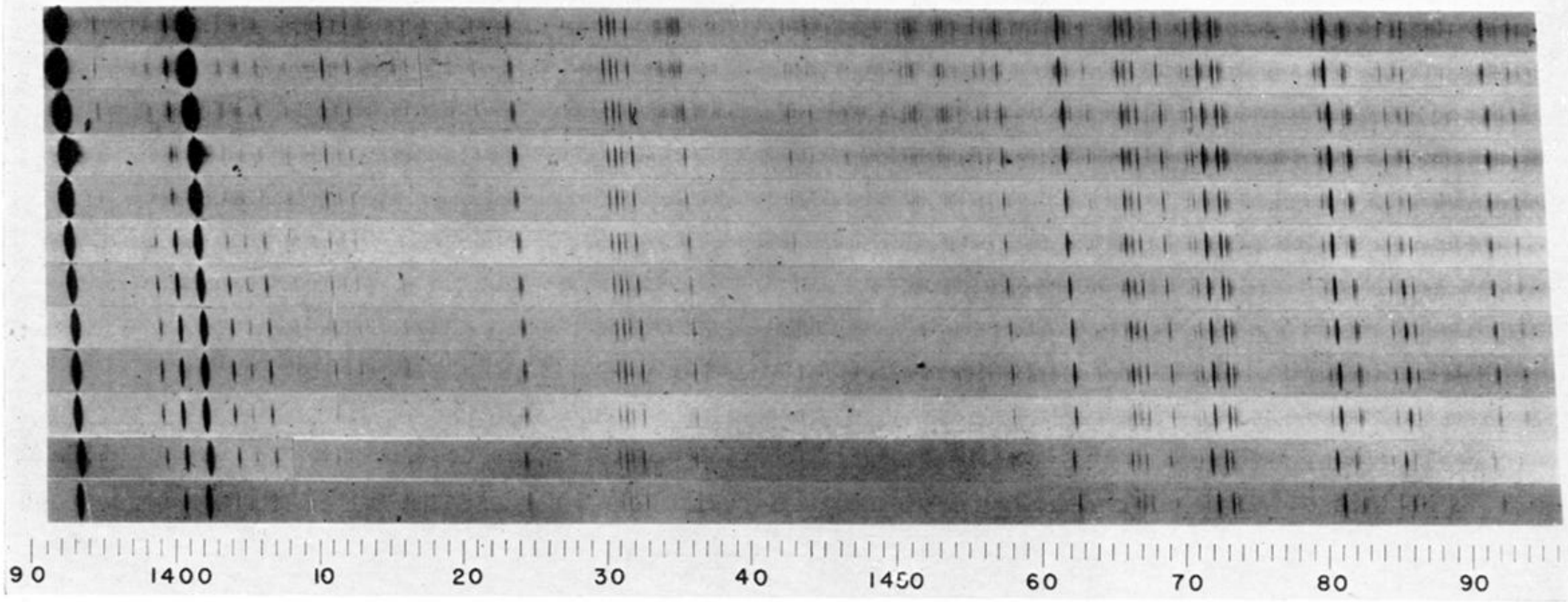

h	min	s
14	11	54
	12	23
	13	35
	14	21
	18	23
	22	26
	26	04
	26	34
	27	47
	28	24
	32	36
	36	39

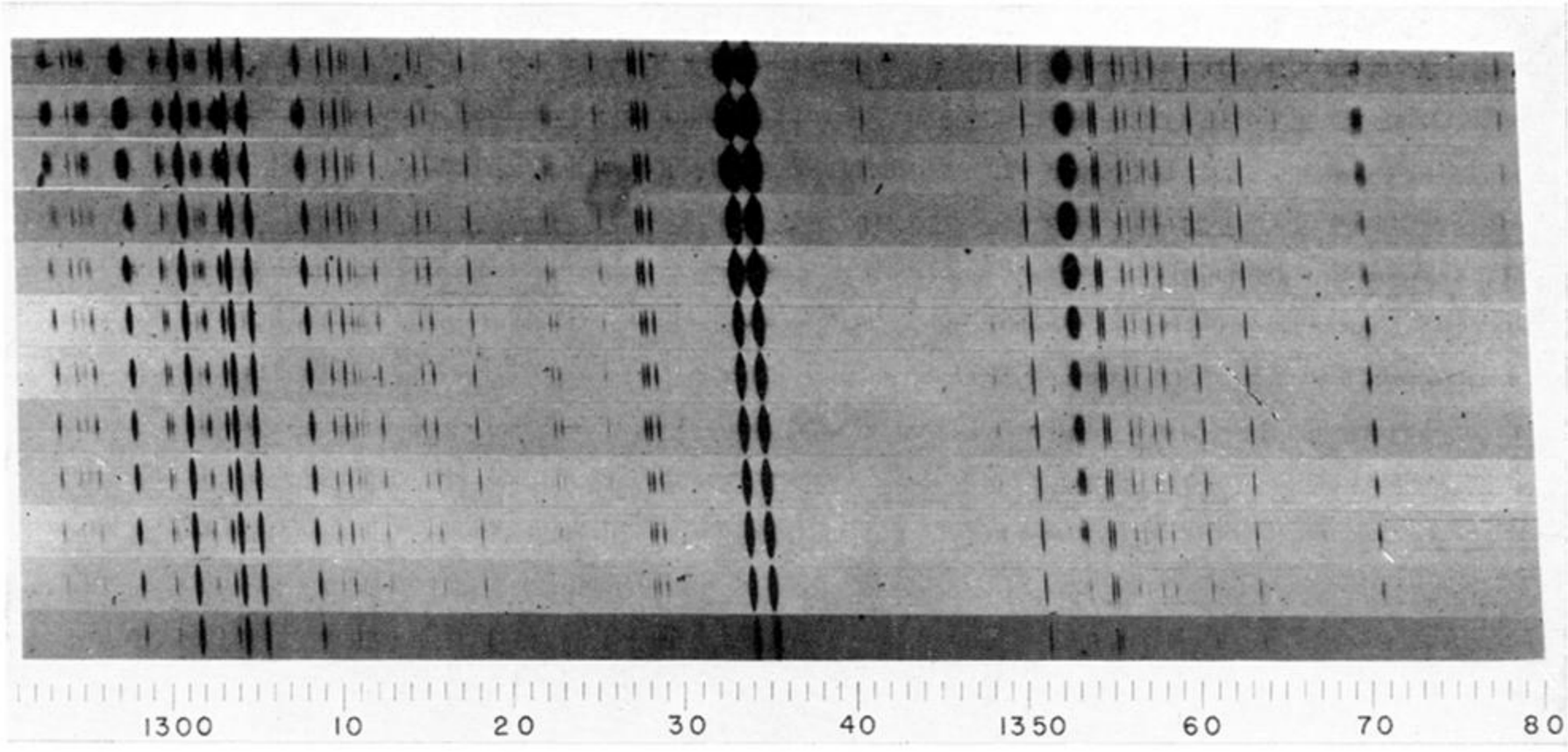

h	min	s
14	11	54
	12	23
	13	35
	14	21
	18	23
	22	26
	26	04
	26	34
	27	47
	28	24
	32	36
	36	39

FIGURE 9. A time sequence of 15 June 1973 flare spectra, wavelength range 1200–1305 Å. The sequence begins with a spectrum, taken during the explosive phase.

FIGURE 10. A time sequence of 15 June 1973 flare spectra, wavelength range 1390–1495 Å.

FIGURE 11. A time sequence of 15 June 1973 flare spectra, wavelength range 1295–1380 Å.

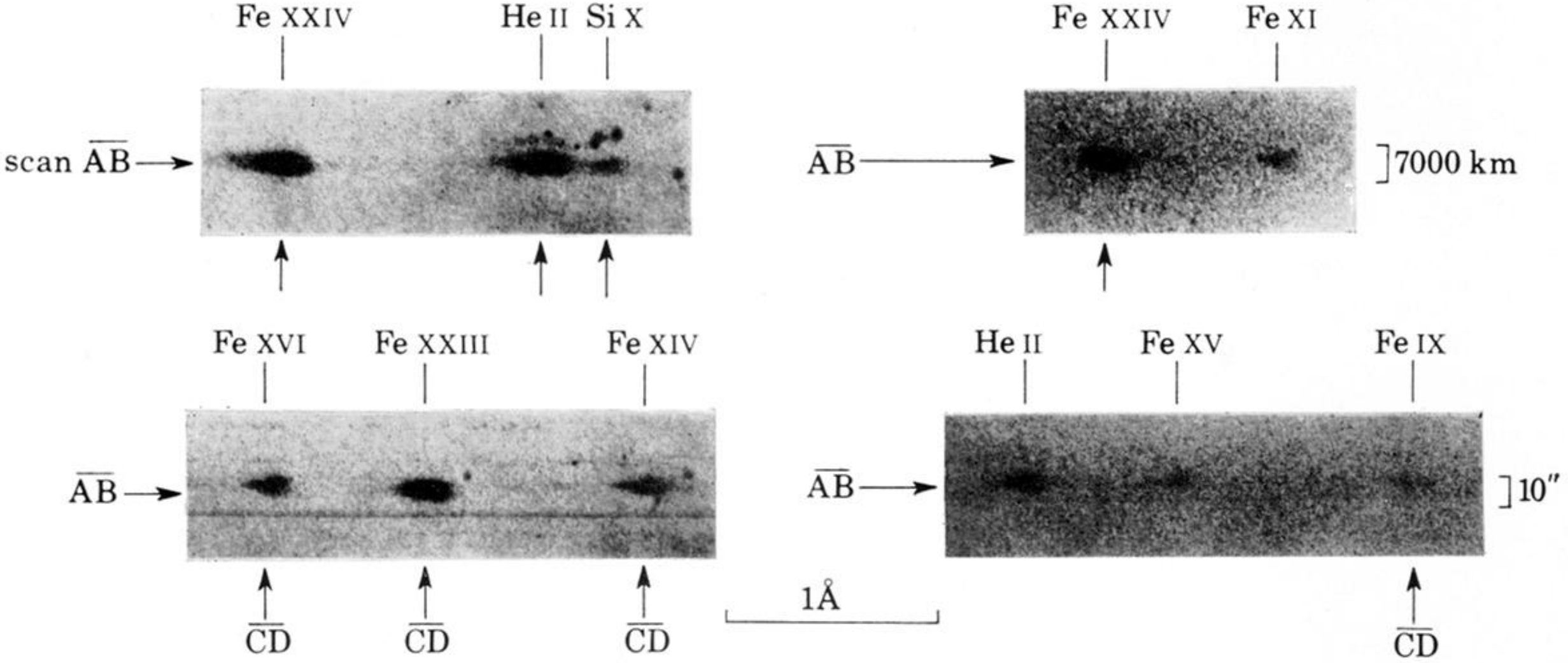

FIGURE 13. The kernel of the 9 August 1973 subflare as photographed on the first plate at 15h53min20s U.T

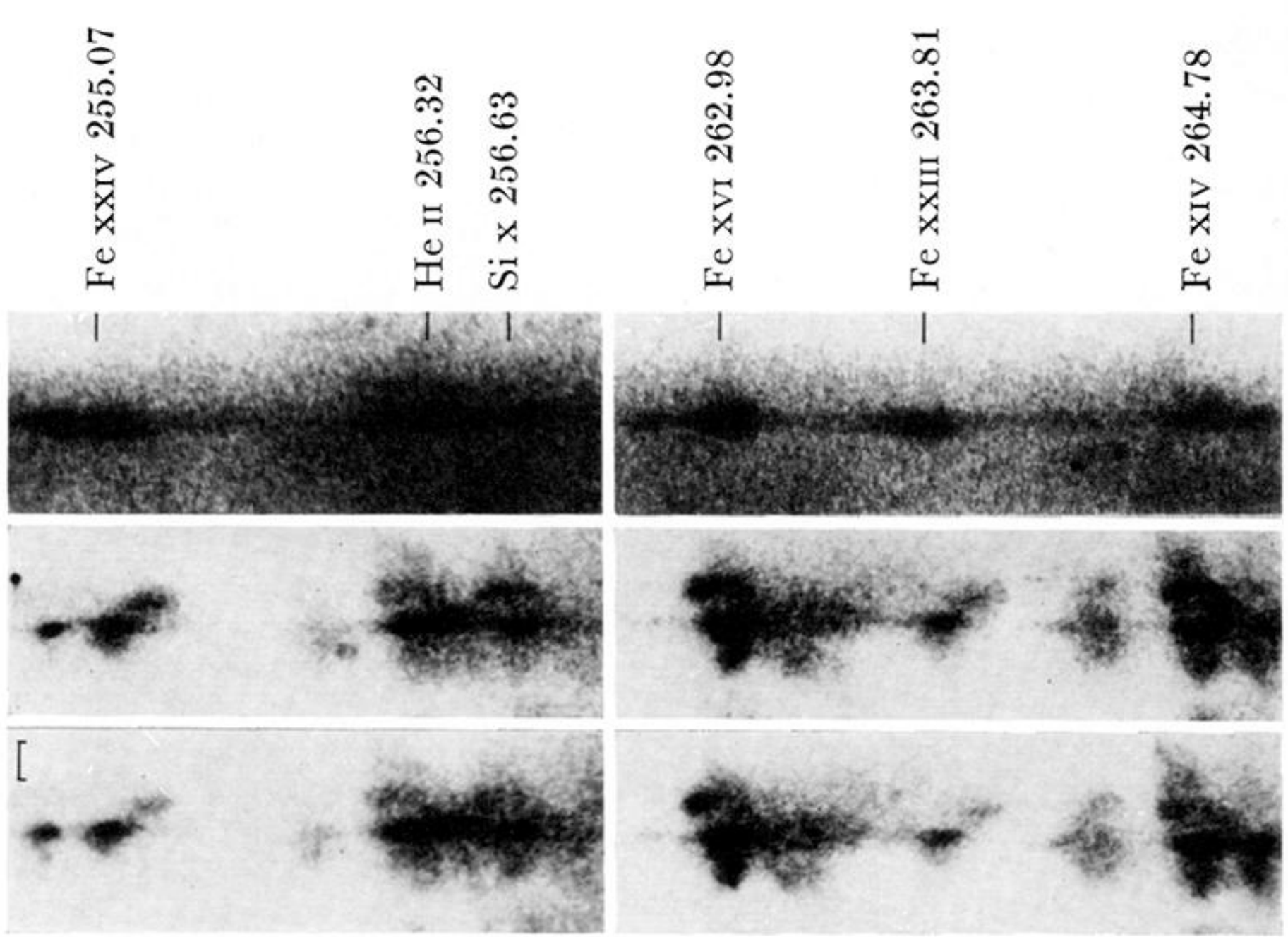

FIGURE 16. Fe XXIII 264 Å and Fe XXIV 255 Å kernels and clouds. Comparison of images of the 9 August 1973 and the 17 December 1973 events.

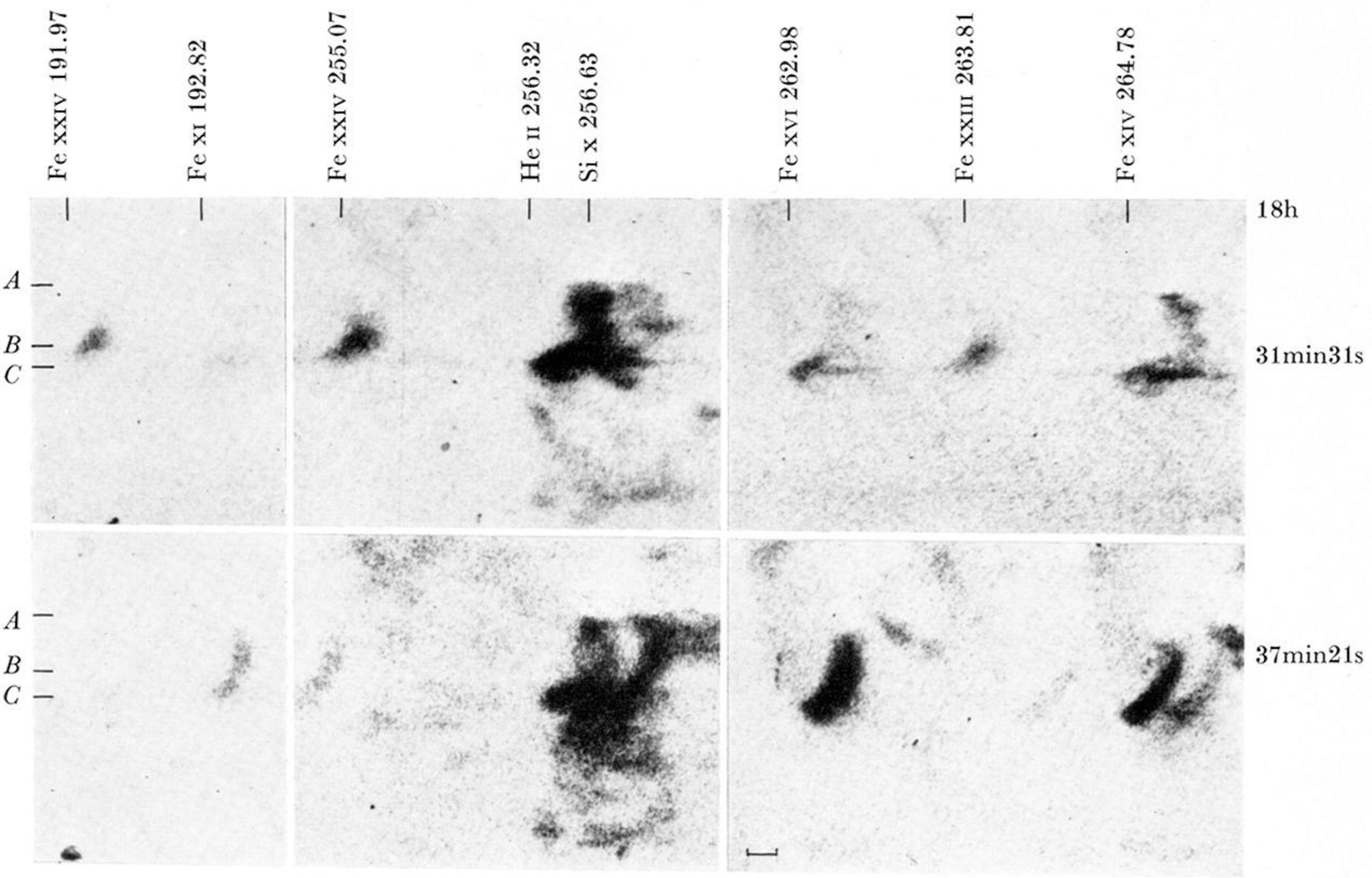

FIGURE 17. Fe XXIII 264 Å, Fe XXIV 192 Å and 255 Å clouds compared with post flare loops in Fe XVI 263 Å and Fe XIV 265 Å as seen in two plates, photographed during a small disk flare on 5 September 1973.

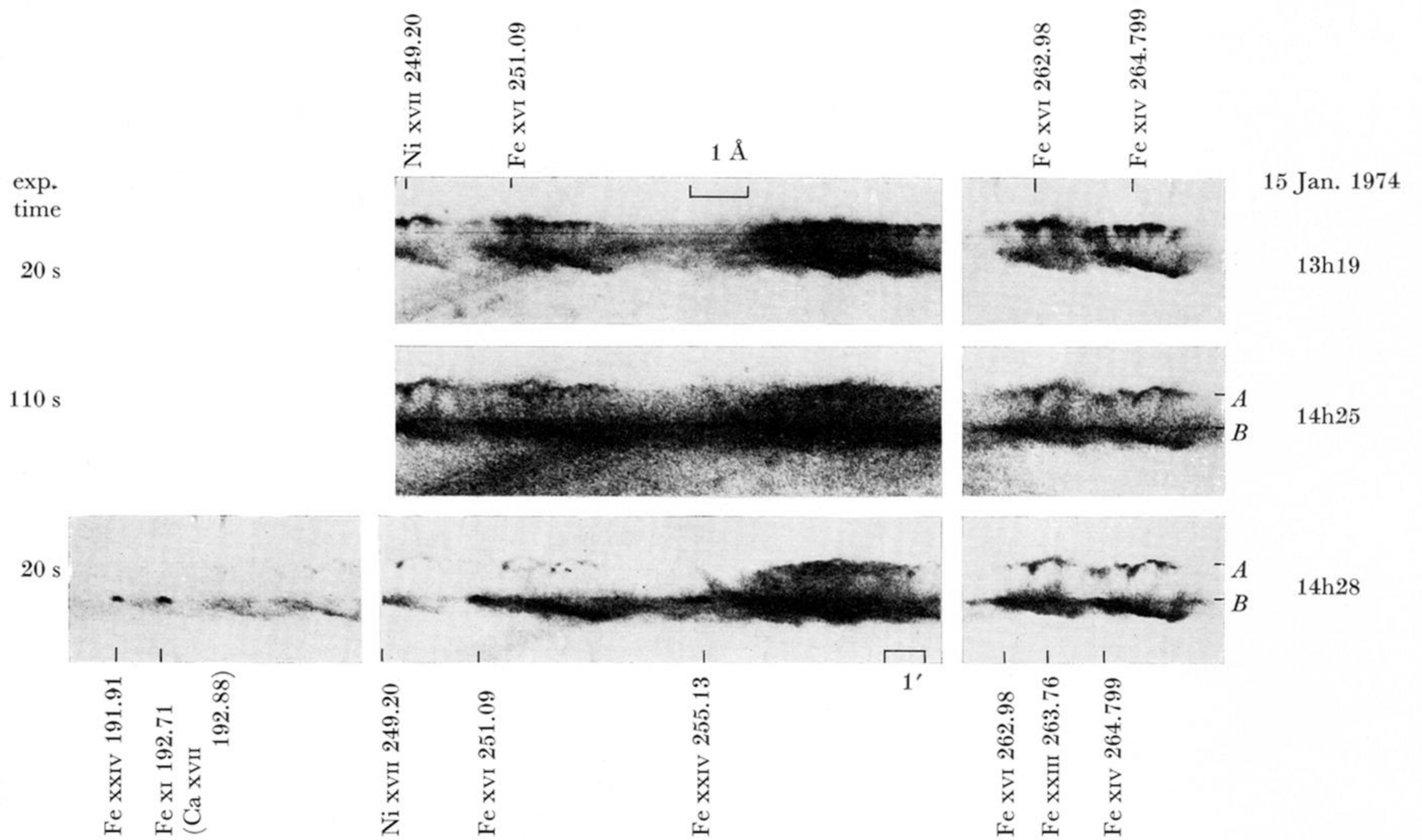

FIGURE 21. Loops, plages and a flare kernel at the limb, 15 January 1974.

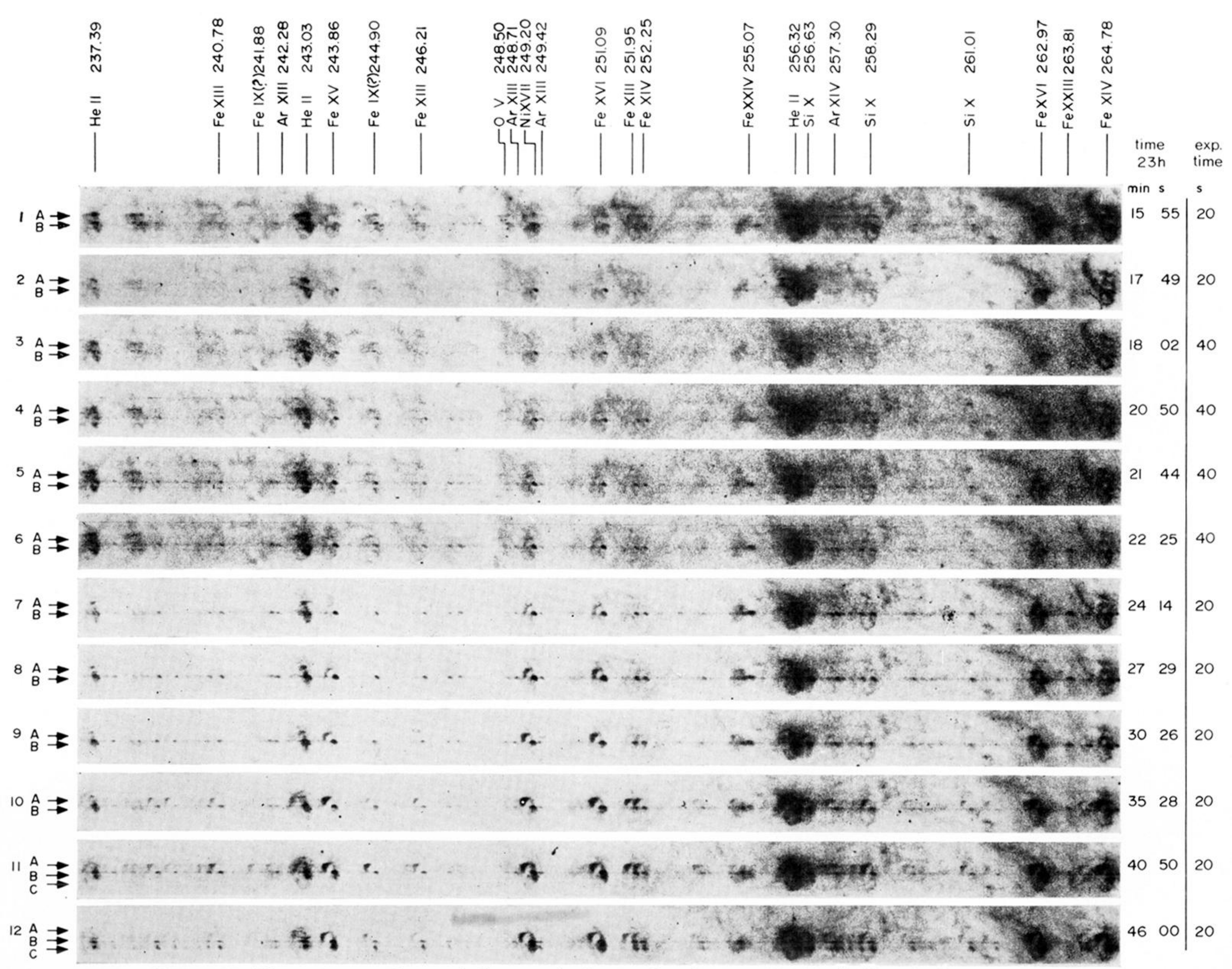

FIGURE 18. Time sequence of spectroheliograms in the wavelength range 237–265 Å. Flare 21 January 1974.

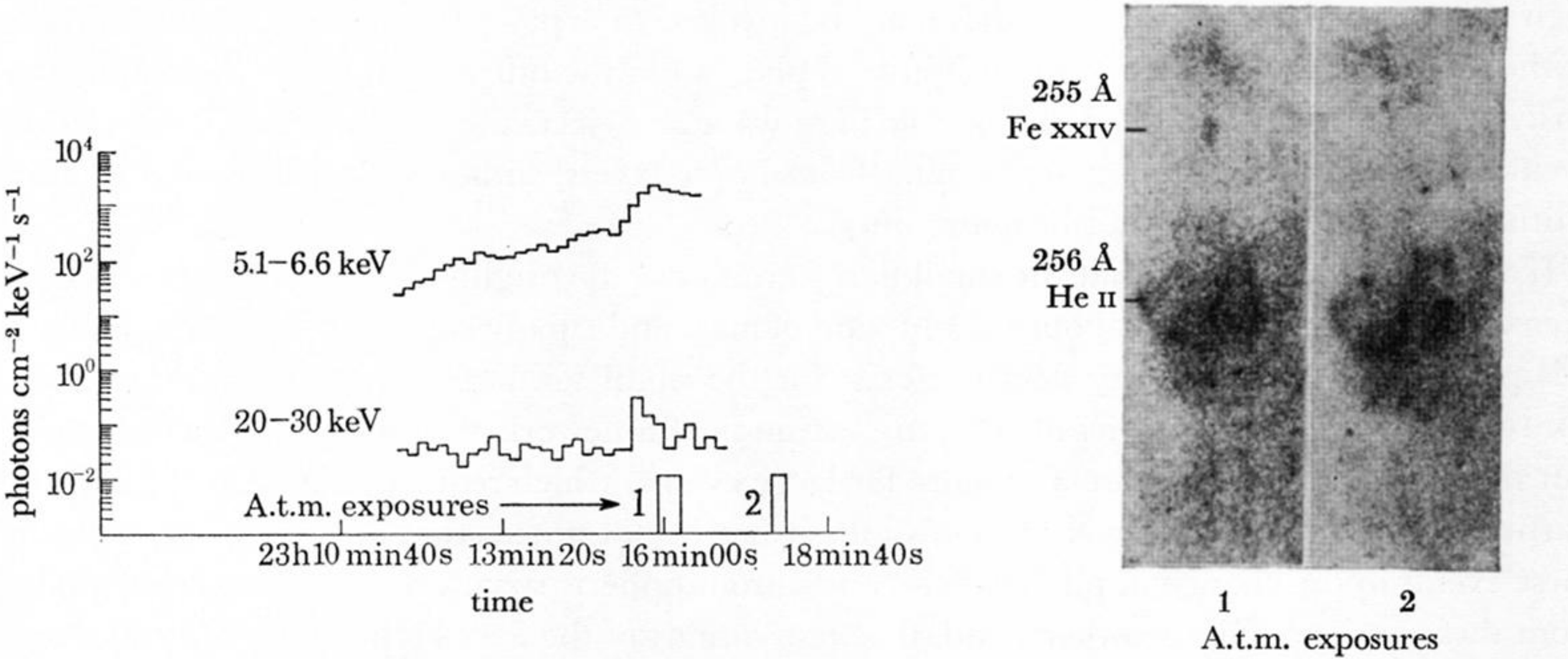

FIGURE 20. Correlation of the 20–30 keV X-ray burst (University of California, OSO-7 X-ray spectrometer) with Fe XXIV 255 Å images.